Theory of amplifier-noise evasion in an oscillator employing a nonlinear resonator

B. Yurke, D. S. Greywall, A. N. Pargellis, and P. A. Busch
AT&T Bell Laboratories, Murray Hill, New Jersey 07974
(Received 7 November 1994)

Resonators driven into self-oscillation via active feedback often form the basis of clocks and other sensitive measurement instrumentation. The phase stability of such an oscillator is ultimately limited by the noise associated with the resonator's intrinsic losses. However, it is often the case that amplifier noise is the dominant cause of the oscillator's phase diffusion. Here it is shown that when the resonator possesses a suitable nonlinearity, the phase diffusion due to amplifier noise can be suppressed, allowing one to achieve a long-term phase stability comparable to the ultimate noise limit.

PACS number(s): 42.50.Ne, 05.40.+j, 06.20.Dk, 03.65.Bz

I. INTRODUCTION

Oscillators based on resonators maintained in self-oscillation via active feedback are of tremendous technological importance. Included are devices such as lasers and masers, and a variety of radio-frequency and low-frequency oscillators. Not only are these used for time keeping and signal generation, but they also often provide the basis for other types of sensitive and precise measurement techniques [1, 2]. The long-term phase or frequency stability of such devices is, in principle, ultimately determined by noise associated with loss mechanisms intrinsic to the resonator itself. However, amplifier noise also contributes to phase diffusion and can be, in some circumstances, the dominant source of frequency jitter. It is shown in this paper that even when the feedback amplifier or gain medium is very noisy, oscillators employing resonators with suitable reactive nonlinearities can exhibit a long-term phase stability comparable to that characteristic of the resonator's loss.

The presence of a cubic nonlinearity in the resonator's restoring force causes a distortion of the resonance curve away from the purely Lorentzian line shape. This distortion takes the form of a pulling of the frequency, and at sufficiently large drives, leads to a resonance curve that is a multivalued function of the frequency. Consequently, there are frequencies where the slope of the amplitude-versus-frequency curve is infinite. The drive at which the resonance curve first exhibits a single point of infinite slope is referred to as the critical drive and this point as the critical point. The phase difference between the response and the drive exhibits points of infinite slope at the same frequencies, and so here the oscillation frequency is insensitive to the phase of the drive. A resonator operated at a point of infinite slope therefore might be expected to be immune to fluctuations in the feedback signal. Indeed, it is demonstrated in this paper that an oscillator employing phase feedback can exhibit enhanced long-term phase stability even though short-term stability remains unchanged.

The method described here for enhancing an oscillator's long-term phase stability provides a nondemolition method for tracking a resonator's phase. In a subsequent manuscript [3] a quantum analysis will be presented demonstrating that the technique, in fact, provides a quantum-nondemolition method [4, 5] of tracking this phase. That back-action evasion or squeezed-state techniques could be used to enhance the performance of an oscillator was recognized by Caves [6]. For work on electromechanical systems in which squeezing or back-action evasion is employed to reduce the noise of quantities other than the phase or frequency, the reader is directed to Refs. [7] and [8].

A schematic of the oscillator circuit studied is depicted in Fig. 1. It consists of a resonator coupled to an amplifier. The output of the amplifier is fed into a phase shifter and then into an amplitude limiter before being returned to the resonator as its drive. It will be shown that this oscillator is stable at all operating points which are set by adjusting the phase and the amplitude of the limiter's output. In particular, stable operation is achieved at the special points on the resonance curve where the slope is infinite. The bulk of this paper is devoted to the analysis of the noise behavior of this oscillator specialized to the case of the particular mechanical resonator that was used to provide an experimental demonstration of the general concepts [2]. A schematic of the silicon beam resonator is given in Fig. 2.

The root-mean-square deviation δf of the measured frequency away from the mean frequency for an oscillator employing a linear resonator scales as $\tau^{-1/2}$ where τ is the time interval over which the frequency is measured, i.e., the frequency counter time interval. This behavior arises due to the unconstrained random walk of the resonator's phase as it is perturbed by the various sources of noise. Optimum frequency stability is achieved with a linear resonator when it is operated at resonance, i.e., at the peak of the resonance curve. Under conditions for which the amplifier's input port noise and the noise from the limiter are negligible, the long-term behavior of $(\delta f)^2$ can be written in the form

$$(\delta f)^2 = (D_{N2} + D_L)/4\pi^2\tau \ , \tag{1.1}$$

where D_{N2} and D_L are, respectively, the diffusion constants characterizing the diffusion of the oscillator's phase

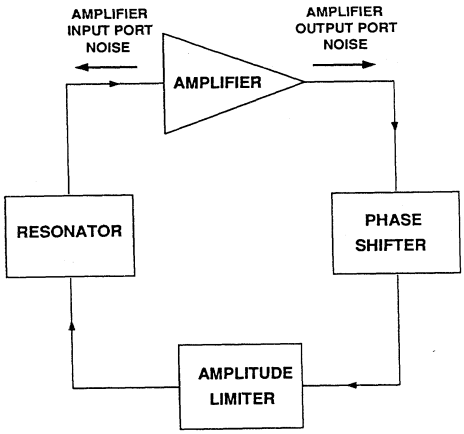

FIG. 1. Schematic of the oscillator analyzed in the manuscript. The oscillator consists of a resonator whose motion is monitored by an amplifier. The output of the amplifier is phase shifted and then passed through an amplitude limiter. The output of the limiter drives the resonator. Arrows are shown indicating the signal flow and the flow of noise both from the amplifier's input port and the output port.

due to the amplifier's output port noise and due to the noise associated with the resonator's intrinsic loss.

For a nonlinear resonator operated at its critical point the expression for the variance in the frequency is

$$(\delta f)^2 = D_L/\pi^2\tau \ . \tag{1.2}$$

The phase diffusion is now independent of amplifier noise and driven entirely by resonator loss noise. The subject of this paper is the derivation of Eqs. (1.1) and (1.2) along with the expressions for the diffusion constants.

The equations of motion governing the various components of the oscillator are presented in Sec. II. In Sec. III the slowly varying envelope approximation is made. In Sec. IV equations of motion are obtained for the amplitude and phase fluctuations of the resonator. In Sec. V the steady state solution is discussed and expressions for the resonator amplitude, the drive amplitude, and detuning frequency at the critical point are obtained. The stability of the oscillator is discussed in Sec. VI. In Sec. VII a general expression for the phase diffusion of the oscillator is obtained. This general expression is specialized to various cases of particular interest in Sec. VIII. Section IX provides a demonstration that the enhanced phase stability can be observed in the signal at the output port of the amplifier even though this signal may be severely contaminated with broadband noise. Finally, in Sec. X various expressions for the mechanical properties of the example beam resonator are derived.

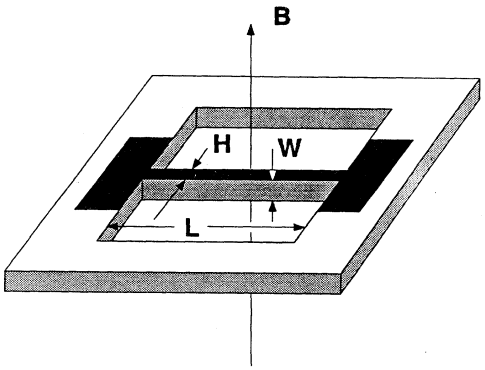

FIG. 2. Mechanical resonator used in the experiments of Ref. [2] with dimensions defined and the direction of the magnetic field B indicated. The beam vibrates transverse to the magnetic field. The black area indicates the region of metallization which provides the path for the drive current. The voltage induced along the conductor is a measure of the resonator's motion.

II. THE SYSTEM

Here we consider a mechanical resonator consisting of a mass M and a spring with a nonlinear restoring force F. This force is given by

$$F = K_1 Y + K_3 Y^3 \ , \tag{2.1}$$

where Y is the displacement of the mass from its equilibrium position.

The resonator's motion is both excited and detected using a scheme that depends on the resonator being located in a uniform magnetic field B. The field, the direction of motion, and a conductor of length ℓ attached to the mass are mutually perpendicular. An alternating current passed through the conductor provides the drive via the Lorentz force. An amplifier of infinite input impedance monitors the electromotive force developed along the moving conductor.

The resonator's equation of motion is

$$M\frac{d^2Y}{dt^2} + \mu_T \frac{dY}{dt} + K_1 Y + K_3 Y^3 = F_D + F_A + F_L \ . \tag{2.2}$$

Here, F_D is the Lorentz force generated by the drive current I_{DS} flowing through the conductor. This force has both coherent and fluctuating components and is given by

$$F_D = \ell B I_{DS} \ . \tag{2.3}$$

F_A is the fluctuating force exerted on the resonator because of current noise I_{AN} emitted from the input port of the amplifier. This Lorentz force is given by

$$F_A = \ell B I_{AN} \ . \tag{2.4}$$

The force F_L is the fluctuating force associated with the resonator's intrinsic loss and can be thought of as a force exerted on the resonator by a dashpot. The constant μ_T is the total damping experienced by the resonator and arises from power loss within the resonator and from power dissipated in the drive current source. Let μ denote the damping constant for the resonator when the drive is disconnected (called the intrinsic resonator loss) and let μ_D denote the damping due to the power loss of the resonator into the drive. The constant for the total damping is then

$$\mu_T = \mu + \mu_D \tag{2.5}$$

with μ_D given by

$$\mu_D = \frac{\ell^2 B^2}{R_D} , \tag{2.6}$$

where the output impedance R_D of the drive is taken to be purely resistive. In this case, in addition to the damping due to internal power loss, the resonator will exhibit damping due to power lost into the output impedance of the drive.

The electromotive force V_R developed across the resonator conductor is given by

$$V_R = \ell B \frac{dY}{dt} . \tag{2.7}$$

This voltage appears across the input port of the amplifier. The voltage V_{out} at the output of the amplifier is

$$V_{out} = G(V_R + V_{AN}) , \tag{2.8}$$

where G is the voltage gain and V_{AN} is the voltage noise (referred to input) appearing at the output port of the amplifier. For simplicity we will assume that this noise is independent of the current noise I_{AN} emitted from the input of the amplifier. To describe the action of the phase shifter and the limiter we write V_{out} in the form

$$V_{out}(t) = V(t)\cos[\Omega t + \phi(t)] , \tag{2.9}$$

where Ω is the self-oscillation frequency, $V(t)$ is a time varying amplitude, and $\phi(t)$ is a time varying phase. The phase shifter shifts the phase of this signal by the amount ϕ_C. Hence, letting V_ϕ denote the voltage at the output of the phase shifter, one has

$$V_\phi(t) = V(t)\cos[\Omega t + \phi(t) + \phi_C] . \tag{2.10}$$

The limiter strips away the time varying amplitude $V(t)$ and replaces it with a constant amplitude. A limiter might be realized by a clipping circuit or a high gain amplifier driven to its rails, or possibly a phase-lock oscillator locked to the phase of its input signal. Hence, the current emitted by the limiter is given by

$$I_{DS} = I_0\cos[\Omega t + \phi(t) + \phi_C] + I_{ND} , \tag{2.11}$$

where I_0 is the constant amplitude and I_{ND} is the fluctuating noise current emitted from the output of the limiter. The constants ϕ_C and I_0 are set by the experimenter and allow the experimenter to choose the system's operating point.

III. THE SLOWLY VARYING ENVELOPE APPROXIMATION

It is now assumed that the resonator has a high quality factor Q. This implies that the damping time is long compared to the period of oscillation and justifies the slowly varying envelope approximation. The quality factor and the damping constant are related by

$$Q = \frac{M\Omega_0}{\mu_T} , \tag{3.1}$$

where the natural frequency of oscillation Ω_0 is

$$\Omega_0 = \sqrt{\frac{K_1}{M}} . \tag{3.2}$$

We write the displacement in the form

$$Y = \frac{1}{\sqrt{2K_1}}[\mathcal{A}(t)e^{-i\Omega t} + \mathcal{A}^*(t)e^{i\Omega t}] , \tag{3.3}$$

where Ω is the drive frequency which in general differs from the natural frequency by a small detuning

$$\omega = \Omega - \Omega_0 . \tag{3.4}$$

The amplitude $\mathcal{A}$ varies slowly on the time scale of the resonator's oscillation period and is normalized so that $|\mathcal{A}|^2$ has units of energy. In fact, the energy stored in a linear resonator is given by

$$\mathcal{E} = |\mathcal{A}|^2 \tag{3.5}$$

as can be verified by substituting Eq. (3.3) into

$$\mathcal{E} = \frac{M}{2}\left(\frac{dY}{dt}\right)^2 + \frac{K_1}{2}Y^2 . \tag{3.6}$$

The current I_{DS} is written in the analogous form

$$I_{DS} = \sqrt{\frac{2}{R_D}}[\mathcal{A}_D^{in}(t)e^{-i\Omega t} + \mathcal{A}_D^{in*}(t)e^{i\Omega t}] . \tag{3.7}$$

Here the normalization has been chosen so that

$$\bar{P}_D^{av} = |\mathcal{A}_D^{in}|^2 \tag{3.8}$$

is the average available power from the drive. This is demonstrated by substituting Eq. (3.7) into the expression for the instantaneous available drive power P_D^{av}

$$P_D^{av} = \frac{R_D I_{DS}^2}{4} \tag{3.9}$$

and performing the time average. The superscript "in" indicates that $|\mathcal{A}_D^{in}|^2$ can be thought of as the power propagating from the drive current source "in" toward the resonator.

Similarly, the current noise I_{AN} is written

$$I_{AN} = \sqrt{\frac{2}{R_D}}[\mathcal{A}_A^{in}(t)e^{-i\Omega t} + \mathcal{A}_A^{in*}(t)e^{i\Omega t}] . \tag{3.10}$$

The time averaged available noise power $\bar{P}_A^{av}$ that the resonator could extract from the amplifier's input in the presence of the drive's output impedance R_D is then

$$\bar{P}_A^{av} = |\mathcal{A}_A^{in}|^2 . \tag{3.11}$$

The fluctuating force exerted by the dashpot on the resonator is written

$$F_L = \sqrt{2\mu}[\mathcal{A}_L^{in}(t)e^{-i\Omega t} + \mathcal{A}_L^{in*}(t)e^{i\Omega t}] . \tag{3.12}$$

The available noise power P_L^{av} from the fluctuating force associated with the dashpot, i.e., the maximum noise power that the resonator could extract from the loss is given by

$$P_L^{av} = \frac{F_L^2}{4\mu} . \tag{3.13}$$

The normalization used in Eq. (3.12) leads to the time averaged available power being given by

$$\bar{P}_L^{av} = |\mathcal{A}_L^{in}|^2 \ . \tag{3.14}$$

The slowly varying envelope approximation is carried out by approximating the second derivative of Y with respect to time as

$$\frac{d^2Y}{dt^2} = -\frac{\Omega_0^2 + 2\Omega_0\omega}{\sqrt{2K_1}}[\mathcal{A}e^{-i\Omega t} + \mathcal{A}^* e^{i\Omega t}] - i\Omega_0\sqrt{\frac{2}{K_1}}\left[\frac{d\mathcal{A}}{dt}e^{-i\Omega t} - \frac{d\mathcal{A}^*}{dt}e^{i\Omega t}\right] \tag{3.15}$$

and by approximating the first derivative of Y by

$$\frac{dY}{dt} = -i\frac{\Omega_0}{\sqrt{2K_1}}[\mathcal{A}e^{-i\Omega t} - \mathcal{A}^* e^{i\Omega t}] \ . \tag{3.16}$$

In addition, since a high Q resonator will suppress all oscillations except those close to Ω_0, Y^3 will be approximated as

$$Y^3 = \frac{3|\mathcal{A}|^2}{(2K_1)^{3/2}}[\mathcal{A}e^{-i\Omega t} + \mathcal{A}^* e^{i\Omega t}] \ . \tag{3.17}$$

Substituting Eqs. (2.4) and (2.3) into Eq. (2.2) and substituting Eqs. (3.3), (3.7), (3.10), (3.12), and Eqs. (3.15)–(3.17) into the resulting equation one obtains the following equation for $\mathcal{A}$:

$$\frac{d\mathcal{A}}{dt} + \left(\frac{1}{\tau_T} - i\omega\right)\mathcal{A} + i\gamma|\mathcal{A}|^2\mathcal{A} = i\sqrt{\frac{2}{\tau_D}}\mathcal{A}_D^{in} + i\sqrt{\frac{2}{\tau_D}}\mathcal{A}_A^{in} + i\sqrt{\frac{2}{\tau_L}}\mathcal{A}_L^{in} \ . \tag{3.18}$$

Here the constant gamma is defined by

$$\gamma = \frac{3K_3}{4M^{1/2}K_1^{3/2}} \ . \tag{3.19}$$

The amplitude ring-down times τ_T, τ_L, and τ_D are given by

$$\tau_T = \frac{2M}{\mu_T} \ , \tag{3.20}$$

$$\tau_L = \frac{2M}{\mu} \ , \tag{3.21}$$

and

$$\tau_D = \frac{2MR_D}{\ell^2 B^2} \ . \tag{3.22}$$

From Eqs. (2.5) and (2.6) it follows that the ring-down time τ_D due to power loss into the drive and the ring-down time τ_L due to power dissipated internally in the resonator are related to the total amplitude ring-down time τ_T through

$$\frac{1}{\tau_T} = \frac{1}{\tau_L} + \frac{1}{\tau_D} \ . \tag{3.23}$$

Writing V_R as

$$V_R = \hat{V}_R e^{-i\Omega t} + \hat{V}_R^* e^{i\Omega t} \ , \tag{3.24}$$

it follows, from Eqs. (2.7) and (3.16), that

$$\hat{V}_R = -i\frac{\ell B}{\sqrt{2M}}\mathcal{A} \ . \tag{3.25}$$

Writing V_{out} and V_{AN} as

$$V_{out} = \hat{V}_{out}e^{-i\Omega t} + \hat{V}_{out}^* e^{i\Omega t} \tag{3.26}$$

and

$$V_{AN} = \hat{V}_{AN}e^{-i\Omega t} + \hat{V}_{AN}^* e^{i\Omega t} \tag{3.27}$$

one obtains from Eq. (2.8)

$$\hat{V}_{out} = G(\hat{V}_R + \hat{V}_{AN}) \ . \tag{3.28}$$

Decomposing V_ϕ into the form

$$V_\phi = \hat{V}_\phi e^{-i\Omega t} + \hat{V}_\phi^* e^{i\Omega t} \ , \tag{3.29}$$

the action of the phase shifter, Eq. (2.10) can be expressed as

$$\hat{V}_\phi = e^{i\phi_C}\hat{V}_{out} \ . \tag{3.30}$$

Equation (2.11) can now be written

$$I_{DS} = \frac{I_0}{2}\frac{\hat{V}_\phi}{|\hat{V}_\phi|}e^{-i\Omega t} + \frac{I_0}{2}\frac{\hat{V}_\phi^*}{|\hat{V}_\phi|}e^{i\Omega t} + I_{ND} \ . \tag{3.31}$$

Decomposing the drive noise current I_{ND} according to

$$I_{ND} = \sqrt{\frac{2}{R_D}}[\mathcal{A}_{ND}^{in}e^{-i\Omega t} + \mathcal{A}_{ND}^{in*}e^{i\Omega t}] \tag{3.32}$$

and using Eq. (3.7), Eq. (3.31) yields

$$\mathcal{A}_D^{in} = \frac{I_0}{2}\sqrt{\frac{R_D}{2}}\frac{\hat{V}_\phi}{|\hat{V}_\phi|} + \mathcal{A}_{ND}^{in} \ . \tag{3.33}$$

Substituting consecutively Eqs. (3.30), (3.28), and (3.25) into Eq. (3.33) one finally obtains

$$\mathcal{A}_D^{in} = e^{i\phi_C}\frac{I_0}{2}\sqrt{\frac{R_D}{2}}\frac{(\mathcal{A} + i\sqrt{2M}\hat{V}_{AN}/\ell B)}{|\mathcal{A} + i\sqrt{2M}\hat{V}_{AN}/\ell B|} + \mathcal{A}_{ND}^{in} \ . \tag{3.34}$$

This equation and Eq. (3.18) constitute the major results of this section. Equation (3.18) is the equation of motion describing the behavior of the resonator. Equation (3.34) describes the action of the feedback loop.

IV. LINEARIZATION ABOUT THE STEADY STATE SOLUTION

To deal with the complexities of Eqs. (3.18) and (3.34) we linearize about the steady state solution corresponding to the system devoid of noise. Such a procedure is appropriate when the noise induced fluctuations are small compared to the amplitude of oscillation. We thus write the amplitude $\mathcal{A}$ in the form

$$\mathcal{A} = [A + a(t)]e^{i[\phi_0 + \phi(t)]} \ , \tag{4.1}$$

where

$$\mathcal{A}_S = Ae^{i\phi_0} \tag{4.2}$$

is the steady state solution and a and ϕ are, respectively, the small fluctuating components of the amplitude and the phase. To linear order in ϕ, Eq. (4.1) can be written as

$$\mathcal{A} = (A + a + iA\phi)e^{i\phi_0} \ . \tag{4.3}$$

We consider two cases: (1) when feedback from the amplifier is interrupted and the drive emits a sinusoidal current at the frequency Ω and (2) when the feedback loop is closed.

For the open loop case the drive signal is taken to have the form

$$\mathcal{A}_D^{in} = \frac{I_0}{2}\sqrt{\frac{R_D}{2}}e^{i\phi_C} + \mathcal{A}_{DN}^{in} \ . \tag{4.4}$$

Substituting this equation and Eq. (4.3) into Eq. (3.18) one obtains the equations for the steady state solution and for the fluctuating components. In particular, for the steady state solution one has

$$\left(\frac{1}{\tau_T} - i\omega + i\gamma A^2\right) A = ie^{i(\phi_C - \phi_0)} f \ , \tag{4.5}$$

where

$$f = \frac{I_0}{2}\sqrt{\frac{R_D}{\tau_D}} \ . \tag{4.6}$$

Before displaying the equations for the fluctuations it is useful to introduce the following notations:

$$\Gamma_{D1} = \frac{1}{\sqrt{2}}[\mathcal{A}_{DN}^{in}e^{-i\phi_0} + \mathcal{A}_{DN}^{in*}e^{i\phi_0}] \ , \tag{4.7}$$

$$\Gamma_{D2} = -\frac{i}{\sqrt{2}}[\mathcal{A}_{DN}^{in}e^{-i\phi_0} - \mathcal{A}_{DN}^{in*}e^{i\phi_0}] \ , \tag{4.8}$$

$$\Gamma_{A1} = \frac{1}{\sqrt{2}}[\mathcal{A}_{A}^{in}e^{-i\phi_0} + \mathcal{A}_{A}^{in*}e^{i\phi_0}] \ , \tag{4.9}$$

$$\Gamma_{A2} = -\frac{i}{\sqrt{2}}[\mathcal{A}_{A}^{in}e^{-i\phi_0} - \mathcal{A}_{A}^{in*}e^{i\phi_0}] \ , \tag{4.10}$$

$$\Gamma_{L1} = \frac{1}{\sqrt{2}}[\mathcal{A}_{L}^{in}e^{-i\phi_0} + \mathcal{A}_{L}^{in*}e^{i\phi_0}] \ , \tag{4.11}$$

and

$$\Gamma_{L2} = -\frac{i}{\sqrt{2}}[\mathcal{A}_{L}^{in}e^{-i\phi_0} - \mathcal{A}_{L}^{in*}e^{i\phi_0}] \ . \tag{4.12}$$

The equations for the fluctuations about the steady state can now be written

$$\frac{da}{dt} + \frac{1}{\tau_T}a + (\omega - \gamma A^2)A\phi = -\frac{1}{\sqrt{\tau_D}}\Gamma_{D2} - \frac{1}{\sqrt{\tau_D}}\Gamma_{A2} - \frac{1}{\sqrt{\tau_L}}\Gamma_{L2} \tag{4.13}$$

and

$$A\frac{d\phi}{dt} + \frac{1}{\tau_T}A\phi - (\omega - 3\gamma A^2)a = \frac{1}{\sqrt{\tau_D}}\Gamma_{D1} + \frac{1}{\sqrt{\tau_D}}\Gamma_{A1} + \frac{1}{\sqrt{\tau_L}}\Gamma_{L1} \ . \tag{4.14}$$

Equations (4.5), (4.13), and (4.14) constitute the open loop results.

We now consider the closed loop case. The linearization of Eq. (3.34) can be accomplished by using Eq. (4.3) to write

$$\frac{(\mathcal{A} + i\sqrt{2M}\hat{V}_{AN}/\ell B)}{|(\mathcal{A} + i\sqrt{2M}\hat{V}_{AN}/\ell B)|} = e^{i\phi_0}\frac{(A + \Gamma)}{|A + \Gamma|} \ , \tag{4.15}$$

where

$$\Gamma = a + iA\phi + ie^{-i\phi_0}\sqrt{2M}\hat{V}_{AN}/\ell B \ . \tag{4.16}$$

Since the magnitude of Γ is regarded as small compared to the mean field A one can write

$$\frac{(A + \Gamma)}{|A + \Gamma|} = 1 + \frac{\Gamma - \Gamma^*}{2A} \ . \tag{4.17}$$

Introducing the quantity $\bar{V}_{AN}$ defined by

$$\bar{V}_{N1} = \frac{1}{\sqrt{2}}[\hat{V}_{AN}e^{-i\phi_0} + \hat{V}_{AN}^*e^{i\phi_0}] \tag{4.18}$$

and using Eq. (3.22), Eq. (4.17) can be written

$$\frac{(A + \Gamma)}{|A + \Gamma|} = 1 + i\phi + \frac{i}{A}\sqrt{\frac{\tau_D}{2R_D}}\bar{V}_{N1} \ . \tag{4.19}$$

Substituting this equation into Eq. (4.15) and substituting the result into Eq. (3.34) yields the following expression for the linearized feedback:

$$\mathcal{A}_D^{in} = e^{i(\phi_C + \phi_0)}\frac{I_0}{2}\sqrt{\frac{R_D}{2}}\left(1 + i\phi + \frac{i}{A}\sqrt{\frac{\tau_D}{2R_D}}\bar{V}_{N1}\right) + \mathcal{A}_{ND}^{in} \ . \tag{4.20}$$

The phase jitter ϕ_A of the drive caused by the amplifier output noise is thus given by

$$\phi_A = \frac{1}{A}\sqrt{\frac{\tau_D}{2R_D}}\bar{V}_{N1} \ . \tag{4.21}$$

By substituting Eq. (4.3) and Eq. (4.20) into Eq. (3.18) equations for the steady state and for the fluctuations about the steady state are obtained. The equation for the steady state, using Eq. (4.6), is

$$\left(\frac{1}{\tau_T} - i\omega + i\gamma A^2\right) A = ie^{i\phi_C} f \ . \tag{4.22}$$

Except for the absence of the phase ϕ_0 this equation is the same as Eq. (4.5) derived for the open loop case. The fact that ϕ_0 no longer appears is a reflection of the time translation symmetry possessed by the self-excited oscillator. The drive of an externally driven resonator breaks this symmetry.

The equations of motion for the fluctuating quantities, using Eqs. (4.7) – (4.12) and using Eq. (4.22) to eliminate $e^{i\phi_C}$, become

$$\frac{da}{dt}+\frac{1}{\tau_T}a=\sqrt{\frac{\tau_D}{2R_D}}(\omega-\gamma A^2)\bar{V}_{N1}-\frac{1}{\sqrt{\tau_D}}\Gamma_{D2} -\frac{1}{\sqrt{\tau_D}}\Gamma_{A2}-\frac{1}{\sqrt{\tau_L}}\Gamma_{L2} \tag{4.23}$$

and

$$A\frac{d\phi}{dt}-(\omega-3\gamma A^2)a=\frac{1}{\tau_T}\sqrt{\frac{\tau_D}{2R_D}}\bar{V}_{N1}+\frac{1}{\sqrt{\tau_D}}\Gamma_{D1} +\frac{1}{\sqrt{\tau_D}}\Gamma_{A1}+\frac{1}{\sqrt{\tau_L}}\Gamma_{L1}\ . \tag{4.24}$$

V. STEADY STATE SOLUTION

Here we derive properties of the steady state behavior of the system. Since Eqs. (4.5) and (4.22) describing the steady state behavior for the open loop and closed loop configurations are the same except for the different phase variables appearing in the exponential function, the solutions for both systems are the same, apart from a relabeling of the phase. Taking the square of the norm of both sides of Eq. (4.22) and introducing

$$E=A^2 \tag{5.1}$$

one obtains the cubic equation in E

$$E^3-\frac{2\omega}{\gamma}E^2+\left(\frac{\omega^2}{\gamma^2}+\frac{1}{\gamma^2\tau_T^2}\right)E-\frac{f^2}{\gamma^2}=0\ . \tag{5.2}$$

This equation in general will have three roots with only the real roots carrying physical significance. The solutions to cubic equations of the form of Eq. (5.2) are known [9] and are repeated here for completeness and convenience. It is useful to introduce the quantities

$$p=-\frac{2\omega}{\gamma}\ , \tag{5.3}$$

$$q=\frac{\omega^2}{\gamma^2}+\frac{1}{\gamma^2\tau_T^2}\ , \tag{5.4}$$

and

$$r=-\frac{f^2}{\gamma^2}\ . \tag{5.5}$$

From these quantities we construct

$$R=\frac{p^2-3q}{9} \tag{5.6}$$

and

$$S=\frac{2p^3-9pq+27r}{54}\ . \tag{5.7}$$

When $S^2-R^3>0$, Eq. (5.2) has only one real solution which is given by

$$E=-\mathrm{sgn}(S)\left[(\sqrt{S^2-R^3}+|S|)^{1/3} +\frac{R}{(\sqrt{S^2-R^3}+|S|)^{1/3}}\right]-\frac{p}{3}\ . \tag{5.8}$$

When $R^3-S^2\geq 0$, Eq. (5.2) has three real roots. Introducing the quantity

$$\theta=\arccos(S/\sqrt{R^3})\ , \tag{5.9}$$

the roots can be written as

$$E_1=-2\sqrt{R}\cos\left(\frac{\theta}{3}\right)-\frac{p}{3}\ , \tag{5.10}$$

$$E_2=-2\sqrt{R}\cos\left(\frac{\theta+2\pi}{3}\right)-\frac{p}{3}\ , \tag{5.11}$$

and

$$E_3=-2\sqrt{R}\cos\left(\frac{\theta+4\pi}{3}\right)-\frac{p}{3}\ . \tag{5.12}$$

Once A has been determined through Eq. (5.1) and Eqs. (5.3)–(5.12), one can determine the phase ϕ_C using Eq. (4.22). Separating Eq. (4.22) into real and imaginary parts one obtains

$$\frac{A}{\tau_T}=-f\sin\phi_C \tag{5.13}$$

and

$$(\omega-\gamma A^2)A=-f\cos\phi_C\ . \tag{5.14}$$

These two equations then yield

$$\cot\phi_C=\tau_T(\omega-\gamma A^2) \tag{5.15}$$

which is easily inverted to yield ϕ_C. Another useful relation follows from taking the derivative of Eq. (5.15) with respect to ω, namely

$$\frac{\partial\phi_C}{\partial\omega}=-\frac{\tau_T(1-\gamma\partial E/\partial\omega)}{1+\tau_T^2(\omega-\gamma E)^2}\ . \tag{5.16}$$

We now derive expressions for the phase and the amplitude at special points along the resonance curve. First we consider the peak of the resonance. At this point, with the drive held fixed,

$$\frac{\partial E}{\partial\omega}=0\ . \tag{5.17}$$

The derivative of Eq. (5.2) with respect to ω yields

$$\frac{\partial E}{\partial\omega}=-\frac{2\tau_T^2(\omega-\gamma E)E}{1+\tau^2(\omega-\gamma E)(\omega-3\gamma E)} \tag{5.18}$$

which, with Eq. (5.17), implies that at the peak of the resonance

$$\omega-\gamma A^2=0\ . \tag{5.19}$$

Substituting this equation into Eq. (4.22) one finds that $\cos\phi_C=0$. From this and Eq. (4.22) it also follows that the relation between the amplitude A and the drive f is

$$A=\tau_T f \tag{5.20}$$

and that the phase angle ϕ_C is

$$\phi_C=-\pi/2\ . \tag{5.21}$$

Substituting Eqs. (5.17)–(5.19) into Eq. (5.16) one also

obtains

$$\frac{\partial \phi_C}{\partial \omega} = -\tau_T \ . \tag{5.22}$$

Note that Eqs. (5.19) through (5.22) hold even in the linear case when $\gamma = 0$. This suggests that behavior at resonance of a nonlinear resonator is similar to that of a linear resonator. For the case of phase diffusion of the oscillator due to amplifier output port noise, the behavior of the system with a nonlinear resonator is in fact identical to that for the corresponding linear resonator, as will be shown in Sec. VIII. For an experimentalist this provides a convenient way of calibrating the performance of an oscillator with a nonlinear resonator against that expected for the corresponding linear resonator operated at resonance.

We now consider points on the resonance curve having infinite slope, that is, points at which

$$\frac{\partial \omega}{\partial E} = 0 \ . \tag{5.23}$$

Note that according to Eq. (5.16) at these points we also have

$$\frac{\partial \omega}{\partial \phi_C} = 0 \ , \tag{5.24}$$

that is, the phase as a function of frequency has infinite slope at the same frequency at which the resonance curve does. These points of infinite slope occur, see Eq. (5.18), when

$$\frac{1}{\tau_T^2} + (\omega - \gamma A^2)(\omega - 3\gamma A^2) = 0 \ . \tag{5.25}$$

One operating point is of particular interest. This is the critical point where in addition to Eq. (5.23) one has

$$\frac{\partial^2 \omega}{\partial E^2} = 0 \ . \tag{5.26}$$

Taking the reciprocal of both sides of Eq. (5.18), differentiating with respect to E, and using Eqs. (5.23), (5.25), and (5.26) we have

$$E = \frac{2\omega}{3\gamma} \ . \tag{5.27}$$

Substituting this into Eq. (5.25), using Eq. (5.1), one obtains for the critical point detuning

$$\omega = \frac{\sqrt{3}}{\tau_T} \ , \tag{5.28}$$

where here and throughout the rest of the paper, it is assumed that $\gamma \geq 0$. Combining this relation with Eq. (5.27) yields for the critical point amplitude

$$E_c = \frac{2\sqrt{3}}{3\gamma\tau_T} \ . \tag{5.29}$$

Equations (5.2), (5.28), and (5.29) then lead to the expression for the critical point drive, namely

$$f^2 = \frac{8\sqrt{3}}{9\gamma\tau_T^3} \ . \tag{5.30}$$

Substituting Eqs. (5.28)–(5.30) into Eqs. (5.13) and (5.14) one finds that at the critical point

$$\phi_C = -\frac{2\pi}{3} \ . \tag{5.31}$$

For the critical point drive, Eq. (5.30), Eqs. (5.1) and (5.20) yield, for the square of the amplitude at the peak of the resonance curve, the expression

$$E_m = \frac{8\sqrt{3}}{9\gamma\tau_T} \ . \tag{5.32}$$

Comparing this with Eq. (5.29) one sees that for the critical drive the ratio of the amplitude A_c at the critical point to the amplitude A_m at the peak of the resonance curve is given by

$$\frac{A_c}{A_m} = \frac{\sqrt{3}}{2} \ . \tag{5.33}$$

We have found this equation helpful in experimentally locating the critical point of a resonator.

Figure 3 displays a set of resonance curves for various values of the drive generated using Eqs. (5.3)–(5.12) and the parameters $\gamma = 1$ and $\tau_T = 1$. The amplitude A is plotted normalized with respect to the maximum amplitude A_m attained at the critical drive. The curve labeled 1.0 is for the critical drive $f_c^2 = 8\sqrt{3}/9$, see Eq. (5.30). The curve labeled 2.0 corresponds to $f^2 = 2f_c^2$ and the curve labeled 0.5 to $f^2 = 0.5f_c^2$. Frequency pulling of the resonance curves due to the nonlinearity is evident at all three drives. The critical point on the critical drive curve is indicated by a small gap in the resonance curve. At smaller drives the resonance curves are single valued; at larger drives they are multivalued as a function of frequency and exhibit two points of infinite slope.

Figure 4 displays a similar set of curves for the phase as a function of frequency which were generated using

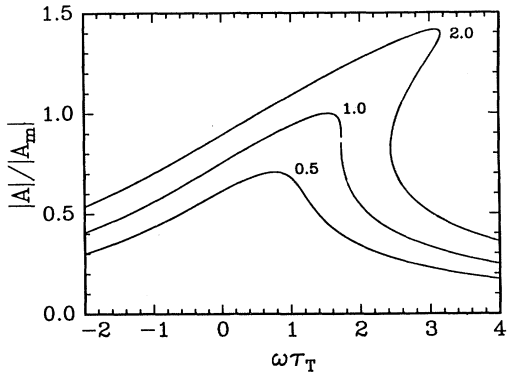

FIG. 3. Sequence of resonance curves for which $\gamma = \tau_T = 1$. The central curve corresponds to the critical drive. For the curves labeled 0.5 and 2.0 the incident drive power is, respectively, half or twice that of the critical drive. At the critical drive the resonance curve exhibits a point of infinite slope, called the critical point. This is indicated by a gap in the curve. For drives larger than the critical drive, the resonance curves are multivalued functions of the detuning frequency ω.

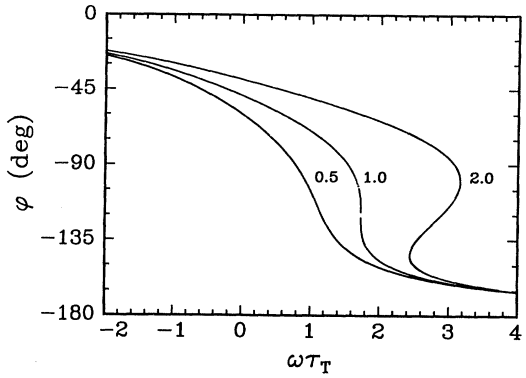

FIG. 4. Sequence showing the phase-versus-detuning-frequency curves corresponding to the resonance curves of Fig. 3. At the critical drive the phase also exhibits a point of infinite slope which occurs at the same value of ω as the critical point for the resonance curve. For drives greater then the critical drive the phase becomes a multivalued function of ω. Note, however, that ω, when viewed as a function of the phase, remains single valued.

Eqs. (5.3)–(5.12) and Eq. (5.15) to extract the phase. Note that the phase curve at the critical drive also exhibits a point of infinite slope at the same value of the detuning as the resonance curve itself. Again the critical point is indicated by a small gap in the curve.

VI. STABILITY

Having described the steady state solutions, we now determine the conditions under which they are stable. First we consider the open loop case. The homogeneous equations associated with Eq. (4.13) and Eq. (4.14) are

$$\frac{da}{dt}+\frac{1}{\tau_T}a+(\omega-\gamma A^2)A\phi=0 \tag{6.1}$$

and

$$A\frac{d\phi}{dt}+\frac{1}{\tau_T}A\phi-(\omega-3\gamma A^2)a=0\ . \tag{6.2}$$

Combining these to eliminate a we have

$$\frac{d^2\phi}{dt}+\frac{2}{\tau_T}\frac{d\phi}{dt}+\left[\frac{1}{\tau_T^2}+(\omega-\gamma A^2)(\omega-3\gamma A^2)\right]\phi=0\ . \tag{6.3}$$

Writing ϕ as

$$\phi=\phi_0 e^{-\lambda t} \tag{6.4}$$

leads to the secular equation

$$\lambda^2-\frac{2}{\tau_T}\lambda+\left[\frac{1}{\tau_T^2}+(\omega-\gamma A^2)(\omega-3\gamma A^2)\right]=0 \tag{6.5}$$

which has the roots

$$\lambda_\pm=\frac{1}{\tau_T}\pm i\sqrt{(\omega-\gamma A^2)(\omega-3\gamma A^2)}\ . \tag{6.6}$$

The steady state solution is unstable if the real part of either of the roots is negative. This occurs when

$$-(\omega-\gamma A^2)(\omega-3\gamma A^2)>\frac{1}{\tau_T^2}\ . \tag{6.7}$$

When

$$-(\omega-\gamma A^2)(\omega-3\gamma A^2)=\frac{1}{\tau_T^2} \tag{6.8}$$

one of the roots of the secular equation is zero and the other is negative; so the system is neutrally stable. Instability occurs when the resonance curve is multivalued and is manifested by bistability and hysteresis effects as the frequency is swept back and forth through this multivalued region.

We now consider the closed loop case. The homogeneous versions of Eqs. (4.23) and (4.24) are

$$\frac{da}{dt}+\frac{1}{\tau_T}a=0 \tag{6.9}$$

and

$$A\frac{d\phi}{dt}-(\omega-3\gamma A^2)a=0\ . \tag{6.10}$$

Eliminating a from these two equations one obtains

$$\frac{d^2\phi}{dt^2}+\frac{1}{\tau_T}\frac{d\phi}{dt}=0\ . \tag{6.11}$$

The secular equation is now

$$\lambda^2-\frac{1}{\tau_T}\lambda=0 \tag{6.12}$$

with the roots

$$\lambda_1=0 \tag{6.13}$$

and

$$\lambda_2=1/\tau_T\ . \tag{6.14}$$

We thus see that in the closed loop case the steady state solution is always stable. The damping time of the amplitude and the settling time of the phase is τ_T. The zero eigenvalue results from the neutral stability of the phase which is a manifestation of the time translation symmetry exhibited by the equations of motion of a self-excited oscillator. That the system with feedback should exhibit enhanced stability can be inferred directly from Fig. 4, which shows that the detuning, when regarded as a function of ϕ_c, is single valued. Since it is the phase that is the control parameter being fed back to the resonator the oscillator's frequency should settle to the unique value determined by the phase setting of the phase shifter.

VII. DIFFUSION OF THE RESONATOR'S PHASE

The quantity $\langle[\phi(t+\tau)-\phi(t)]^2\rangle$, where the brackets $\langle\ \rangle$ denote ensemble averaging, measures the extent to which the resonator's phase diffuses in the time interval τ. This is the quantity evaluated in this section.

To begin, we introduce the Fourier transforms

$$\tilde{a}(\xi) = \frac{1}{\sqrt{2\pi}} \int_{-\infty}^{\infty} dt e^{i\xi t} a(t) \ , \tag{7.1}$$

$$\tilde{\phi}(\xi) = \frac{1}{\sqrt{2\pi}} \int_{-\infty}^{\infty} dt e^{i\xi t} \phi(t) \ , \tag{7.2}$$

$$\tilde{V}_{N2}(\xi) = \frac{1}{\sqrt{2\pi}} \int_{-\infty}^{\infty} dt e^{i\xi t} \bar{V}_{N2}(t) \ , \tag{7.3}$$

and

$$\tilde{\Gamma}_{D1}(\xi) = \frac{1}{\sqrt{2\pi}} \int_{-\infty}^{\infty} dt e^{i\xi t} \Gamma_{D1}(t) \ . \tag{7.4}$$

The Fourier transforms of the Langevin noise terms, Γ_{D2}, Γ_{A1}, Γ_{A2}, Γ_{L1}, and Γ_{L2} are defined in analogy with Eq. (7.4). With the Fourier transform of the phase defined by Eq. (7.2) one can show

$$\langle [\phi(t+\tau) - \phi(t)]^2 \rangle = \frac{1}{2\pi} \int_{-\infty}^{\infty} d\xi \int_{-\infty}^{\infty} d\xi' e^{-i(\xi+\xi')t} \times (e^{-i\xi\tau} - 1)(e^{-i\xi'\tau} - 1) \times \langle \tilde{\phi}(\xi)\tilde{\phi}(\xi') \rangle \ . \tag{7.5}$$

The quantity $\langle \tilde{\phi}(\xi)\tilde{\phi}'(\xi') \rangle$ is straightforward to compute: taking the Fourier transform of Eq. (4.23) one obtains

$$\tilde{a}(\xi) = \sqrt{\frac{\tau_D}{2R_D}} \frac{(\omega - \gamma A^2)}{(-i\xi + 1/\tau_T)} \tilde{V}_{N1}(\xi) - \frac{\tilde{\Gamma}_{D2}(\xi)}{\sqrt{\tau_D}(-i\xi + 1/\tau_T)} - \frac{\tilde{\Gamma}_{A2}(\xi)}{\sqrt{\tau_D}(-i\xi + 1/\tau_T)} - \frac{\tilde{\Gamma}_{L2}(\xi)}{\sqrt{\tau_L}(-i\xi + 1/\tau_T)} \ . \tag{7.6}$$

Taking the Fourier transform of Eq. (4.24) and then substituting Eq. (7.6) into the resulting equation, one obtains upon rearrangement

$$\tilde{\phi}(\xi) = \frac{i}{\xi A} \sqrt{\frac{\tau_D}{2R_D}} \left[\frac{1}{\tau_T} + \frac{(\omega - \gamma A^2)(\omega - 3\gamma A^2)}{-i\xi + 1/\tau_T} \right] \tilde{V}_{N1}(\xi) + \frac{i}{\xi A\sqrt{\tau_D}} [\tilde{\Gamma}_{D1}(\xi) + \tilde{\Gamma}_{A1}(\xi)] - \frac{i}{\xi A\sqrt{\tau_D}} \frac{(\omega - 3\gamma A^2)}{(-i\xi + 1/\tau_T)} \times [\tilde{\Gamma}_{D2}(\xi) + \tilde{\Gamma}_{A2}(\xi)] + \frac{i}{\xi A\sqrt{\tau_L}} \tilde{\Gamma}_{L1}(\xi) - \frac{i}{\xi A\sqrt{\tau_L}} \frac{(\omega - 3\gamma A^2)}{(-i\xi + 1/\tau_T)} \tilde{\Gamma}_{L2}(\xi) \ . \tag{7.7}$$

In order to evaluate the quantity $\langle \tilde{\phi}(\xi)\tilde{\phi}'(\xi') \rangle$ it is necessary to specify the statistical properties of the Langevin noise sources $\tilde{V}_{N1}(\xi)$, $\tilde{\Gamma}_{D1}(\xi)$, $\tilde{\Gamma}_{D2}(\xi)$, $\tilde{\Gamma}_{A1}(\xi)$, $\tilde{\Gamma}_{A2}(\xi)$, $\tilde{\Gamma}_{L1}(\xi)$, and $\tilde{\Gamma}_{L2}(\xi)$. The noise sources will be taken to have zero mean, that is,

$$\langle \tilde{V}_{N1}(\xi) \rangle = \langle \tilde{\Gamma}_{D1}(\xi) \rangle = \langle \tilde{\Gamma}_{D2}(\xi) \rangle = \langle \tilde{\Gamma}_{A1}(\xi) \rangle = \langle \tilde{\Gamma}_{A2}(\xi) \rangle = \langle \tilde{\Gamma}_{L1}(\xi) \rangle = \langle \tilde{\Gamma}_{L2}(\xi) \rangle = 0 \ . \tag{7.8}$$

We also choose each of these noise sources to be statistically independent, that is, for two distinct noise sources such as $\tilde{\Gamma}_{D1}(\xi)$ and $\tilde{\Gamma}_{D2}(\xi)$ one has

$$\langle \tilde{\Gamma}_{D1}(\xi)\tilde{\Gamma}_{D2}(\xi) \rangle = 0 \ . \tag{7.9}$$

The voltage noise $\tilde{V}_{N1}(\xi)$ is taken to satisfy

$$\langle \tilde{V}_{N1}(\xi)\tilde{V}_{N1}(\xi') \rangle = \frac{v_{rms}^2}{4} \delta(\xi + \xi') \ . \tag{7.10}$$

This corresponds to white voltage noise fluctuations for which the root-mean-square voltage fluctuation per root Hertz is v_{rms}.

The drive noise sources $\tilde{\Gamma}_{D1}(\xi)$ and $\tilde{\Gamma}_{D2}(\xi)$ are taken to have the following expectation values:

$$\langle \tilde{\Gamma}_{D1}(\xi)\tilde{\Gamma}_{D1}(\xi') \rangle = \langle \tilde{\Gamma}_{D2}(\xi)\tilde{\Gamma}_{D2}(\xi') \rangle = \frac{\eta_D}{2} \delta(\xi + \xi') \ . \tag{7.11}$$

This corresponds to a white noise source whose available power has a flat power spectrum. η_D is the noise power per unit bandwidth.

Similarly, the expectation values for the amplifier's input port noise sources $\tilde{\Gamma}_{A1}$ and $\tilde{\Gamma}_{A2}$ are taken to be

$$\langle \tilde{\Gamma}_{A1}(\xi)\tilde{\Gamma}_{A1}(\xi') \rangle = \langle \tilde{\Gamma}_{A2}(\xi)\tilde{\Gamma}_{A2}(\xi') \rangle = \frac{\eta_A}{2} \delta(\xi + \xi') \ , \tag{7.12}$$

where η_A is the noise power per unit bandwidth for the amplifier's input port noise that is available to the resonator in the presence of the drive load resistor R_D.

The intrinsic loss noise sources are also taken to have expectation values of the form

$$\langle \tilde{\Gamma}_{L1}(\xi)\tilde{\Gamma}_{L1}(\xi') \rangle = \langle \tilde{\Gamma}_{L2}(\xi)\tilde{\Gamma}_{L2}(\xi') \rangle = \frac{\eta_L}{2} \delta(\xi + \xi') \ , \tag{7.13}$$

where η_L is the noise power per unit bandwidth for the noise available from the loss.

For white noise sources the total power diverges. One is, nevertheless, justified in making the approximation Eq. (4.17) since the noise is filtered by the response of the resonator which manifests itself via the filter functions given in Eqs. (7.6) and (7.7). The resonator, therefore, only responds to noise within a bandwidth of order $1/2\pi\tau_T$ about the resonant frequency.

From the inverse transform of the Fourier transform Eq. (7.2), using (7.7) and (7.8), it is readily shown that the mean of the two-time phase difference is zero, that is,

$$\langle \phi(t+\tau) - \phi(t) \rangle = 0 \ . \tag{7.14}$$

The quantity $\langle [\phi(t+\tau) - \phi(t)]^2 \rangle$ is thus the variance in the phase difference and provides a measure of the diffu-

sion of the phase. From Eqs. (7.9)–(7.13) it follows that $\langle\tilde{\phi}(\xi)\tilde{\phi}'(\xi')\rangle$ has the form

$$\langle\tilde{\phi}(\xi)\tilde{\phi}'(\xi')\rangle = \mathcal{B}(\xi)\delta(\xi+\xi') \ , \tag{7.15}$$

where

$$\mathcal{B}(\xi) = \frac{\tau_D v_{rms}^2}{8R_D A^2\xi^2}\left[\left(\frac{1}{\tau_T} + \frac{(\omega-\gamma A^2)(\omega-3\gamma A^2)}{\tau_T(\xi^2+1/\tau_T^2)}\right)^2 + \frac{\xi^2(\omega-\gamma A^2)^2(\omega-3\gamma A^2)^2}{(\xi^2+1/\tau_T^2)^2}\right] + \frac{1}{2A^2\xi^2}\left(\frac{\eta_D+\eta_A}{\tau_D}+\frac{\eta_L}{\tau_L}\right)\left(1+\frac{(\omega-3\gamma A^2)^2}{\xi^2+1/\tau_T^2}\right) . \tag{7.16}$$

From this equation it is evident that

$$\mathcal{B}(\xi) = \mathcal{B}(-\xi) \ . \tag{7.17}$$

Using Eqs. (7.15) and (7.17), Eq. (7.5) becomes

$$\langle[\phi(t+\tau)-\phi(t)]^2\rangle = \frac{4}{\pi}\int_0^\infty d\xi \sin^2(\xi\tau/2)\mathcal{B}(\xi). \tag{7.18}$$

Upon substituting Eq. (7.16) into this equation, the resulting integrals can be evaluated analytically. One obtains

$$\langle[\phi(t+\tau)-\phi(t)]^2\rangle = \frac{\tau_D v_{rms}^2}{8\tau_T^2 R_D A^2}\left\{|\tau| + 2\tau_T^2(\omega-\gamma A^2)(\omega-3\gamma A^2)[|\tau|-\tau_T(1-e^{-|\tau|/\tau_T})] + \tau_T^4(\omega-\gamma A^2)^2(\omega-3\gamma A^2)^2[|\tau|-\tau_T(1-e^{-|\tau|/\tau_T})]\right\} + \frac{1}{2A^2}\left(\frac{\eta_D+\eta_A}{\tau_D}+\frac{\eta_L}{\tau_L}\right)\left\{|\tau| + \tau_T^2(\omega-3\gamma A^2)^2[|\tau|-\tau_T(1-e^{-|\tau|/\tau_T})]\right\} . \tag{7.19}$$

Expressions for the amplitude fluctuations are now obtained. From the inverse of the Fourier transform Eq. (7.1) it is easily shown using Eqs. (7.6) and (7.8) that the fluctuating amplitude $a(t)$ has zero mean

$$\langle a(t)\rangle = 0 \ . \tag{7.20}$$

From Eq. (4.1) it is now a straightforward exercise to show that the variance in the amplitude fluctuations is given by

$$(\Delta\mathcal{A})^2 \equiv \langle\mathcal{A}^2\rangle - \langle\mathcal{A}\rangle^2 = \langle a^2(t)\rangle \ . \tag{7.21}$$

The quantity $\sqrt{\langle a^2(t)\rangle}$ is thus a measure of the amplitude fluctuations. This quantity can be obtained from the two-time correlation function $\langle a(t+\tau)a(t)\rangle$. Using Eq. (7.1), one obtains

$$\langle a(t+\tau)a(t)\rangle = \frac{1}{2\pi}\int_{-\infty}^{\infty}d\xi\int_{-\infty}^{\infty}d\xi' e^{-i[\xi(t+\tau)+\xi' t]} \times\langle\tilde{a}(\xi)\tilde{a}(\xi')\rangle \ . \tag{7.22}$$

From Eq. (7.6) and Eqs. (7.10)–(7.13) one obtains

$$\langle\tilde{a}(\xi)\tilde{a}(\xi')\rangle = \left[\frac{\tau_D v_{rms}^2}{8R_D}(\omega-\gamma A^2)^2 + \frac{1}{2}\left(\frac{\eta_D+\eta_A}{\tau_D}+\frac{\eta_L}{\tau_L}\right)\right]\frac{\delta(\xi+\xi')}{\xi^2+1/\tau_T^2} \ . \tag{7.23}$$

Substituting this into Eq. (7.20) and performing the integrations yields

$$\langle a(t+\tau)a(t)\rangle = \left[\frac{\tau_D v_{rms}^2}{4R_D}(\omega-\gamma A^2)^2 + \left(\frac{\eta_D+\eta_A}{\tau_D}+\frac{\eta_L}{\tau_L}\right)\right]\frac{\tau_T}{4}e^{-|\tau|/\tau_T} \ . \tag{7.24}$$

From this equation one sees that the fluctuations in $a(t)$ occur on the time scale τ_T regardless of the resonator's operating point.

VIII. SPECIFIC CASES

Here we consider specific cases of Eq. (7.19). For convenience, we take $\tau > 0$. If one is operating at the peak of the resonance curve, Eq. (5.19) applies, and Eq. (7.19) becomes

$$\langle[\phi(t+\tau)-\phi(t)]^2\rangle = D_{N2}\tau + (D_{N1}+D_D+D_L) \times\left\{\tau + 4\tau_T^2\gamma^2A^4 \times[\tau-\tau_T(1-e^{-\tau/\tau_T})]\right\} , \tag{8.1}$$

where D_{N2}, D_{N1}, D_D, and D_L are, respectively, the diffusion constant for the phase due to amplifier output port noise, amplifier input port noise, noise coming from the drive, and noise due to the resonator's intrinsic loss. These constants are given by

$$D_{N2} = \frac{\tau_D v_{rms}^2}{8\tau_T^2 R_D A^2} \ , \tag{8.2}$$

$$D_{N1} = \frac{\eta_A}{2\tau_D A^2} \ , \tag{8.3}$$

$$D_D = \frac{\eta_D}{2\tau_D A^2} \ , \tag{8.4}$$

$$D_L = \frac{\eta_L}{2\tau_L A^2} \ . \tag{8.5}$$

From Eq. (8.1) and the fact that γ does not appear in Eq. (8.2) it follows that at resonance the phase diffusion due to amplifier output port noise is independent of the strength of the nonlinearity. When the term con-

taining D_{N2} dominates the phase diffusion this observation provides, for the experimentalist, a convenient way of calibrating the noise behavior of an oscillator with a nonlinear resonator against the expected behavior of the system with a corresponding linear resonator operated at resonance.

Using Eqs. (3.22), (3.24), (3.25), and (4.3) one can show

$$A^2 = \frac{\tau_D}{2R_D}\langle V_R^2\rangle \ , \tag{8.6}$$

where $\langle V_R^2\rangle$ is the mean square of the voltage delivered to the input port of the amplifier. In writing this equation we have neglected the amplitude fluctuations of V_R since the linearization procedure assumes that they are small compared to the mean field. Using Eqs. (8.6), (8.2) can be rewritten in terms of experimentally measurable quantities as

$$D_{N2} = \frac{v_{rms}^2}{4\tau_T^2\langle V_R^2\rangle} \ . \tag{8.7}$$

Using Eq. (8.6) and the relation between η_A and the mean-square current per unit bandwidth i_{rms}^2

$$i_{rms}^2 = \frac{\eta_A}{R_D} \ , \tag{8.8}$$

D_{N1} can also be written in the following forms:

$$D_{N1} = \frac{R_D i_{rms}^2}{8\tau_D A^2} = \frac{R_D^2 i_{rms}^2}{4\tau_D^2\langle V_R^2\rangle} \ . \tag{8.9}$$

It should be noted that the noise coming from the drive need consist only of Nyquist noise associated with the output port impedance R_D. At high temperatures, i.e., $k_B T_D \gg \hbar\omega$, this noise is Johnson noise with

$$\eta_D = k_B T_D \ , \tag{8.10}$$

where k_B is Boltzman's constant and T_D is the temperature of the heat bath associated with R_D. Similarly, the noise associated with the resonator's intrinsic loss is characterized by

$$\eta_L = k_B T_L \ , \tag{8.11}$$

where T_L is the temperature of the heat bath associated with the resonator's loss.

We now consider the case where the system is operated at a point where the slope of the resonance curve is infinite. Substituting Eq. (5.25) into Eq. (7.19) one obtains

$$\begin{aligned}\langle[\phi(t+\tau)-\phi(t)]^2\rangle = {} & D_{N2}\tau_T(1-e^{-\tau/\tau_T}) \\ & +(D_{N1}+D_D+D_L) \\ & \times\left\{\tau+\tau_T^2(\omega-3\gamma A^2)^2\right. \\ & \left.\times[\tau-\tau_T(1-e^{-\tau/\tau_T})]\right\} \ .\end{aligned} \tag{8.12}$$

The term containing D_{N2} is due to the amplifier's output noise. Note that this term becomes constant for large values of τ and so does not lead to long-term wandering of the phase. That is, if all the other noise sources were zero the mean-square uncertainty in the phase would reach a constant value $D_{N2}\tau_T$ independent of measurement time for τ large compared to the loaded resonator's damping time. When τ is short compared to τ_T both Eq. (8.1) and Eq. (8.12) reduce to

$$\langle[\phi(t+\tau)-\phi(t)]^2\rangle = (D_{N2}+D_{N1}+D_D+D_L)\tau \ . \tag{8.13}$$

One thus sees that the short-term stability, obtained by operating the resonator at a point where the slope of the resonance curve is infinite, is no better than the short-term stability one would obtain for the same amplitude A when operated at the resonance curve maximum. It is only the long-term stability that can be improved by operating at a point for which the slope of the resonance curve is infinite.

We now argue that, at a point for which the slope of the resonance curve is infinite, one can, in principle, achieve a long-term noise performance that is determined only by the noise power η_L coming from the resonator loss. Note first that τ_D is proportional to R_D by Eq. (3.22). Therefore, D_D, Eq. (8.4), can be made small by making R_D large. Since R_D and τ_D appear as ratios in Eqs. (8.2), (8.6), and (8.9), the diffusion constants D_{N2} and D_{N1} do not change as R_D is increased and A is held fixed. Furthermore, from Eq. (8.5) one sees that D_L does not depend on R_D or τ_D. Consequently, by making R_D sufficiently large, and holding A fixed, D_D can be made negligible compared to D_L and can be neglected in Eq. (8.12). Next, we hold R_D fixed and decrease the magnetic field B. This decreases the coupling between the resonator and the amplifier and between the resonator and the drive. It follows then from Eq. (3.22) that as B is made smaller τ_D increases. So, by making B sufficiently small, D_{N1}, Eq. (8.9), can also be made negligible compared to D_L. That is, by making the coupling between the amplifier and the resonator sufficiently weak the fluctuating force generated by the amplifier's input port current noise can be made small compared to the fluctuating forces generated by the resonator's internal loss.

With the output impedance of the drive sufficiently large and with a sufficiently small coupling through the transducer Eq. (8.12) can be written

$$\begin{aligned}\langle[\phi(t+\tau)-\phi(t)]^2\rangle = {} & D_{N2}\tau_T(1-e^{-\tau/\tau_T}) \\ & +D_L\left\{\tau+\tau_T^2(\omega-3\gamma A^2)^2\right. \\ & \left.\times[\tau-\tau_T(1-e^{-\tau/\tau_T})]\right\} \ .\end{aligned} \tag{8.14}$$

Note that decreasing the magnetic field also causes D_{N2} to become large through its dependence on τ_D. Consequently, the procedure that allows one to diminish D_{N1} also leads to a degraded short-term stability. Nevertheless, it is evident from Eq. (8.14) that the long-term stability of the oscillator is determined by the noise coming from the loss.

It is useful to specialize further and consider the case where the oscillator is operated at the critical point.

Substituting Eq. (5.1), Eq. (5.28), and Eq. (5.29) into Eq. (8.12) one obtains

$$\langle[\phi(t+\tau)-\phi(t)]^2\rangle = D_{N2}\tau_T(1-e^{-\tau/\tau_T}) + (D_{N1}+D_D+D_L) \times[4\tau-3\tau_T(1-e^{-\tau/\tau_T})] . \quad (8.15)$$

As discussed above, by making R_D sufficiently large and B sufficiently small, D_{N1} and D_D can be made negligible compared to D_L. If we also take τ to be sufficiently large Eq. (8.15) reduces to

$$\langle[\phi(t+\tau)-\phi(t)]^2\rangle = 4D_L\tau . \quad (8.16)$$

This result can be compared with the phase stability obtained from Eq. (8.1),

$$\langle[\phi(t+\tau)-\phi(t)]^2\rangle = D_L\tau . \quad (8.17)$$

This is the optimum phase stability that could be obtained if the only noise in the system was that corresponding to the intrinsic loss. Thus, by working at the critical point with a noisy amplifier, a long-term stability can be achieved for which the root-mean-square wandering of the phase is only a factor of 2 worse than that which could be achieved with a linear resonator and a noiseless amplifier. From the relationship between phase diffusion and the variance in the frequency as reported by a frequency counter

$$(\delta f)^2 = \frac{\langle[\phi(t+\tau)-\phi(t)]^2\rangle}{4\pi^2\tau^2} \quad (8.18)$$

it follows that Eq. (8.17) is equivalent to Eq. (1.2) given in Sec. I. Similarly, Eq. (1.1) is equivalent to the long-time limit of Eq. (8.1) for the case when D_{N1} and D_D have been made negligible.

By using Eq. (8.18) to convert the expressions for phase diffusion into those for frequency stability, the rms uncertainty δf in the frequency has been plotted in Fig. 5 as a function of the frequency counter time interval τ obtained from the general expression Eq. (7.19). For these curves $\tau_T = 1$ and $|A|^2 = 2/\sqrt{3}$. The dashed curve and the dotted curve are both for a linear resonator operated at resonance, i.e., $\gamma = 0$ and $\omega = 0$. The dotted curve is that for a hypothetical amplifier with $v_{rms} = 0$. In addition we have taken

$$D_{N1}+D_D+D_L = \frac{\sqrt{3}}{8}\times 10^{-8} . \quad (8.19)$$

This curve would simply represent the noise floor due to phase diffusion driven by the resonator's loss if $D_{N1} = D_D = 0$. The dashed curve includes, in addition to the noise characterized by Eq. (8.19), the amplifier output port noise with a diffusion constant given by

$$D_{N2} = \frac{\sqrt{3}}{2}\times 10^{-4} . \quad (8.20)$$

The solid curve corresponds to operating the oscillator at the critical point with the strengths of the noise sources still being determined by Eq. (8.19) and Eq. (8.20). Here $\gamma = 1$ and $\omega = \sqrt{3}$. For the linear cases, the dashed and dotted curves show δf scaling as $\tau^{-1/2}$ as discussed above. For both short- and long-frequency counter times the solid curve also scales as $\tau^{-1/2}$. There is an intermediate region, however, where it attains a slope of τ^{-1}. The short-term stability is not improved by operating at the critical point, as is evident from the fact that the solid curve approaches the dashed line for small τ. In the intermediate region the long-term frequency stability increases faster for the oscillator being operated at the critical point. The degree of improvement, however, is bounded by the dotted curve. Hence, at very long times the solid curve becomes parallel to the dotted curve but is a factor of 2 larger than the dotted curve. This is the same factor of 2 that was discussed in connection with Eqs. (8.16) and (8.17).

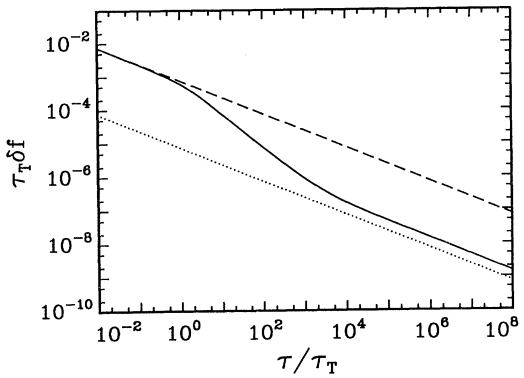

FIG. 5. Frequency stability of the oscillator plotted as a function of the frequency counter time interval. The dotted and dashed curves are for a linear resonator operated at resonance. The dotted curve shows the fundamental noise floor obtained by setting the amplifier output port noise to zero. The solid curve is for the corresponding nonlinear resonator operated at its critical point. Note that the long-time frequency stability of the nonlinear resonator is better than that of the linear amplifier and comes within a factor of 2 of the noise floor. See the text for the parameter values used.

The frequency uncertainty δf as a function of the energy $|A|^2$ stored in the resonator is plotted in Fig. 6 for various fixed values of the frequency counter time. In the plot $|A|^2$ has been normalized with respect to $|A_m|^2$, the maximum value $|A|^2$ attains at the critical drive. The dotted curves are for $\tau = 1$, the dashed curves are for $\tau = 10^3$, and the solid curve is for $\tau = 10^6$. For these plots $\tau_T = 1$. In addition, $D_{N1} = D_D = D_L = 0$ and $D_{N2} = \sqrt{3}/2 \times 10^{-4}$, that is, all noise sources except the amplifier output port noise source have been set to zero. The straight lines scaling as $|A|^{-1}$ are those for the linear resonator at resonance, that is, $\gamma = 0$ and $\omega = 0$. The curves exhibiting minima are for a nonlinear resonator, again $\gamma = 1$ and $\omega = \sqrt{3}$. The parameters were chosen so that when $|A|^2 = 2/\sqrt{3}$ the nonlinear resonator is operated at the critical point. The minima in these curves occur at the critical point. Improvement in frequency stability is realized at those operating points for which these curves fall below their respective linear resonator curves. Since the width of the trough gets nar-

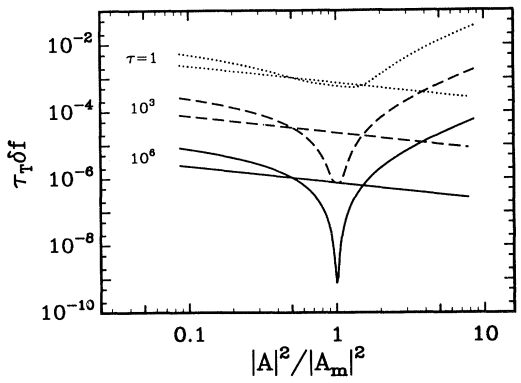

FIG. 6. Frequency stability of the oscillator plotted against the energy stored in the resonator for several values of the frequency counter time interval τ. The straight lines show results for a linear resonator. The curves exhibiting minima are for the corresponding nonlinear resonator. See the text for the parameter values used.

rower as τ increases, one sees that the precision with which $|A|^2$ must be maintained at the critical value becomes more demanding if the greatest noise reduction is to be achieved.

Another meaningful comparison between the nonlinear and linear systems can be made by comparing the critical point stability, Eq. (8.17), with the best phase stability that could be obtained for the linear oscillator with a real amplifier. Since D_{N2} is proportional to $1/B^2$, and D_{N1} is proportional to B^2 there is an optimum magnetic field. The field that minimizes phase diffusion in Eq. (8.1) is given by

$$B^2 = \frac{2Mv_{rms}}{\ell^2\tau_T i_{rms}} \ . \tag{8.21}$$

Upon substituting this into Eq. (8.1) one obtains

$$\langle[\phi(t+\tau)-\phi(t)]^2\rangle = \Big(\frac{v_{rms}i_{rms}}{4\tau_T A^2} + \frac{\eta_D}{2\tau_D A^2} + \frac{\eta_L}{2\tau_L A^2}\Big)\tau \ . \tag{8.22}$$

This can be further optimized by making τ_D very large. In this case the total damping is determined only by resonator loss and one can set $\tau_L = \tau_T$. Equation. (8.22) can now be written

$$\langle[\phi(t+\tau)-\phi(t)]^2\rangle = \frac{v_{rms}i_{rms}+2\eta_L}{4\tau_T A^2}\tau \ . \tag{8.23}$$

Comparing this with Eq. (8.16) leads one to define an improvement factor

$$F = \sqrt{\frac{v_{rms}i_{rms}}{8k_BT_L} + \frac{1}{4}} \ . \tag{8.24}$$

This factor is the ratio of the root-mean-square phase diffusion for an optimized linear system to the root-mean-square long-term phase diffusion for the optimized nonlinear system. When $F > 1$ long-term stability is enhanced using a nonlinear resonator. This condition requires that

$$v_{rms}i_{rms} > 6k_BT_L \ . \tag{8.25}$$

IX. MEASURING THE PHASE

Typically, the resonator's phase is not monitored directly, but instead, is determined using the amplified transducer output, which is generally contaminated with broadband amplifier noise. One method for dealing with this contamination is to insert an appropriate filter between the amplifier's output and the frequency counter.

The voltage V_F delivered to the filter can be written

$$V_F = V_{out} + V_{FN} \ , \tag{9.1}$$

where V_{out} is the amplifier's output signal and V_{FN} is noise that might be added in the process of delivering this signal to the measuring apparatus. This apparatus is taken here to consist of a noiseless filter followed by a noiseless frequency counter. That is, it is assumed that V_F is so large that the noise added by the filter and by the frequency counter can be neglected.

The fluctuating part ϕ_O of the phase of the voltage delivered to the frequency measuring apparatus is

$$\phi_O = \phi + \phi_A + \phi_{FN} \ , \tag{9.2}$$

where ϕ is the resonator's phase, ϕ_A is a fluctuating phase due to the amplifier's output noise, and ϕ_{FN} is a fluctuating phase due to the added noise. The expression for ϕ_A is given in Eq. (4.21). The expression for ϕ_{NF} is given by

$$\phi_{FN} = \frac{1}{GA}\sqrt{\frac{\tau_D}{2R_D}}\tilde{V}_{NF} \ . \tag{9.3}$$

The noise V_{FN} is taken to be statistically independent of all other noise sources and, like Eq. (7.10), is taken to satisfy

$$\langle\tilde{V}_{FM}(\xi)\tilde{V}_{FN}(\xi')\rangle = \frac{v_{FN}^2}{4}\delta(\xi+\xi') \ . \tag{9.4}$$

For simplicity, the transformation performed by the filter on the phase ϕ_O is taken to be

$$\phi_F(t) = \frac{e^{-t/\tau_F}}{\tau_F}\int_{-\infty}^{t} e^{t'/\tau_F}\phi_O(t')dt' \ , \tag{9.5}$$

where τ_F is the filter time constant. This low-pass filter of the phase is causal and has unit response at zero frequency. Substituting the Fourier transform of $\phi_O(t)$ into this equation leads to

$$\phi_F(t) = \frac{1}{\tau_F\sqrt{2\pi}}\int_{-\infty}^{\infty} d\xi \frac{e^{i\xi t}(e^{-i\xi\tau}-1)\tilde{\phi}_0(\xi)}{-i\xi+1/\tau_F} \ . \tag{9.6}$$

From this, one obtains the following expression for the diffusion of the filtered phase:

$$\langle[\phi_F(t+\tau)-\phi_F(t)]^2\rangle = \frac{1}{2\pi\tau_F^2}\int_{-\infty}^{\infty} d\xi \int_{-\infty}^{\infty} d\xi' e^{-i(\xi+\xi')t}\frac{(e^{-i\xi\tau}-1)(e^{-i\xi'\tau}-1)}{(-i\xi+1/\tau_F)(-i\xi'+1/\tau_F)}\langle\tilde{\phi}_O(\xi)\tilde{\phi}_O(\xi')\rangle \ . \tag{9.7}$$

In order to keep track of the origin of various terms in the expressions for the phase diffusion, Eq. (9.2) is temporarily written as

$$\phi_O(t) = \phi + \kappa\phi_A + \phi_{FN} \ . \tag{9.8}$$

The constant κ is merely a label that later will be set to unity. We thus have

$$\begin{aligned}\langle\tilde{\phi}_O(\xi)\tilde{\phi}_O(\xi')\rangle &= \langle\tilde{\phi}(\xi)\tilde{\phi}(\xi')\rangle \\ &+ \kappa[\langle\tilde{\phi}(\xi)\tilde{\phi}_A(\xi')\rangle + \langle\tilde{\phi}_A(\xi)\tilde{\phi}(\xi')\rangle] \\ &+ \kappa^2\langle\tilde{\phi}_A(\xi)\tilde{\phi}_A(\xi')\rangle \\ &+ \langle\tilde{\phi}_{FN}(\xi)\tilde{\phi}_{FN}(\xi')\rangle \ . \end{aligned}\tag{9.9}$$

The expression for $\langle\tilde{\phi}(\xi)\tilde{\phi}(\xi')\rangle$ has already been obtained in Eqs. (7.15) and (7.16). From Eq. (4.21) and Eq. (7.7), using Eq. (7.10), one obtains

$$\langle\tilde{\phi}_A(\xi)\tilde{\phi}(\xi')\rangle + \langle\tilde{\phi}(\xi)\tilde{\phi}_A(\xi')\rangle = \mathcal{C}(\xi)\delta(\xi+\xi'), \tag{9.10}$$

where

$$\mathcal{C}(\xi) = -\frac{\tau_D v_{rms}^2}{4R_D A^2}\frac{(\omega-\gamma A^2)(\omega-3\gamma A^2)}{(\xi^2+1/\tau_T^2)} \ . \tag{9.11}$$

One also obtains

$$\langle\tilde{\phi}_A(\xi)\tilde{\phi}_A(\xi')\rangle = \mathcal{D}(\xi)\delta(\xi+\xi') \tag{9.12}$$

and

$$\langle\tilde{\phi}_{FN}(\xi)\tilde{\phi}_{FN}(\xi')\rangle = \mathcal{E}(\xi)\delta(\xi+\xi') \ , \tag{9.13}$$

where

$$\mathcal{D}(\xi) = \frac{\tau_D v_{rms}^2}{8R_D A^2} \tag{9.14}$$

and

$$\mathcal{E}(\xi) = \frac{\tau_D v_{FN}^2}{8R_D A^2 G^2} \ . \tag{9.15}$$

Since $\mathcal{B}(\xi)$, $\mathcal{C}(\xi)$, $\mathcal{D}(\xi)$, and $\mathcal{E}(\xi)$ are even functions of ξ, Eq. (9.7) can be written in the form

$$\begin{aligned}\langle[\phi_F(t+\tau)-\phi_F(t)]^2\rangle = \frac{4}{\pi\tau_F^2}\int_0^{\infty} d\xi \frac{\sin^2(\xi\tau/2)}{\xi^2+1/\tau_F^2} \\ \times[\mathcal{B}(\xi)+\kappa\mathcal{C}(\xi)+\kappa^2\mathcal{D}(\xi) \\ +\mathcal{E}(\xi)] \ .\end{aligned}\tag{9.16}$$

Upon substituting Eqs. (7.16), (9.11), and (9.14) into this equation the integrals can be performed to yield

$$\begin{aligned}\langle[\phi_F(t+\tau)-\phi_F(t)]^2\rangle = \frac{\tau_D v_{rms}^2}{8\tau_T^2 R_D A^2}\Bigg\{\tau - \tau_F(1-e^{-\tau/\tau_F}) \\ + \left[2\tau_T^2(\omega-\gamma A^2)(\omega-3\gamma A^2)+\tau_T^4(\omega-\gamma A^2)^2(\omega-3\gamma A^2)^2\right] \\ \times\left[\tau - \frac{\tau_F^3(1-e^{-\tau/\tau_F})-\tau_T^3(1-e^{-\tau/\tau_T})}{\tau_F^2-\tau_T^2}\right]\Bigg\} \\ +\frac{1}{2A^2}\left(\frac{\eta_D+\eta_A}{\tau_D}+\frac{\eta_L}{\tau_L}\right)\Bigg\{\tau-\tau_F(1-e^{-\tau/\tau_F}) \\ +\tau_T^2(\omega-3\gamma A^2)^2\left[\tau - \frac{\tau_F^3(1-e^{-\tau/\tau_F})-\tau_T^3(1-e^{-\tau/\tau_T})}{\tau_F^2-\tau_T^2}\right]\Bigg\} \\ -\kappa\frac{\tau_D v_{rms}^2}{4R_D A^2}\tau_T^2(\omega-\gamma A^2)(\omega-3\gamma A^2)\left[\frac{\tau_F(1-e^{-\tau/\tau_F})-\tau_T(1-e^{-\tau/\tau_T})}{\tau_F^2-\tau_T^2}\right] \\ +\kappa^2\frac{\tau_D v_{rms}^2}{8\tau_F R_D A^2}(1-e^{-\tau/\tau_F})+\frac{\tau_D v_{FN}^2}{8\tau_F R_D A^2 G^2}(1-e^{-\tau/\tau_F}) \ .\end{aligned}\tag{9.17}$$

Since the last two terms of this equation are inversely proportional to τ_F, these terms will dominate when τ_F is small and τ is not too large. Thus, to minimize the frequency counter time τ necessary to see the long-term stability enhancement of the oscillator one needs to make τ_F large, i.e., the filter must be narrow band.

When $\tau \gg \tau_T \gg \tau_F$ one obtains

$$\begin{aligned}\langle[\phi_F(t+\tau)-\phi_F(t)]^2\rangle = D_{N2}[1+\tau_T^2(\omega-\gamma A^2)(\omega-3\gamma A^2)]^2\tau + (D_{N1}+D_D+D_L)[1+\tau_T^2(\omega-3\gamma A^2)^2]\tau \\ + D_{N2}\frac{\tau_T^2}{\tau_F} + D_F\frac{\tau_T^2}{\tau_F} \ ,\end{aligned}\tag{9.18}$$

where the diffusion constant D_F is defined by

$$D_F = \frac{\tau_D v_{FN}^2}{8\tau_T^2 R_D A^2 G^2} . \tag{9.19}$$

In the same limit Eq. (7.19) becomes

$$\begin{aligned}\langle[\phi(t+\tau)-\phi(t)]^2\rangle = {} & D_{N2}[1+\tau_T^2(\omega-\gamma A^2) \\ & \times(\omega-3\gamma A^2)]^2\tau \\ & + (D_{N1}+D_D+D_L) \\ & \times[1+\tau_T^2(\omega-3\gamma A^2)^2]\tau . \end{aligned} \tag{9.20}$$

Comparing Eq. (9.18) with Eq. (9.19) one sees that for $\tau \gg \tau_T \gg \tau_F$ the behavior of the phase diffusion reported by the frequency counter is the same as that of the resonator itself, apart from the constant terms $D_{N2}\tau_T^2/\tau_F$ and $D_F\tau_T^2/\tau_F$. The effect of the broadband noise is thus to add a constant to the phase diffusion reported by the frequency counter that is proportional to the filter bandwidth. Hence, for short times τ, the variance in the phase is independent of frequency counter time τ but at sufficiently long times it grows linearly with τ. From the relation between phase diffusion and frequency uncertainty, Eq. (8.18), it thus follows that the δf reported by the frequency counter will decrease as τ^{-1} at short times and then cross over to a falloff proportional to $\tau^{-1/2}$.

This behavior is clearly shown in the plots of δf as a function of τ in Fig. 7. The curves are generated from Eq. (9.17). The parameters are the same as those for the corresponding curves of Fig. 5. In addition, $D_F = 0$ and $\tau_F = 0.01$. The dotted curve is again the linear case without amplifier output port noise and sets the fundamental noise floor. This curve scales as $\tau^{-1/2}$. The dashed curve is for the linear oscillator with amplifier noise. At short times this curve scales as τ^{-1} due to the broadband amplifier output port noise; at long times the curve scales as $\tau^{-1/2}$ due to the intrinsic phase diffusion of the oscillator. This long time behavior matches that of Fig. 5. The solid curve shows results for the resonator operated at the critical point. Although for short times this curve now scales as τ^{-1}, it eventually develops a $\tau^{-1/2}$ time dependence and comes within a factor of 2 of the intrinsic noise floor set by the dotted curve.

As the time interval τ for frequency counting is increased, more prefiltering can be tolerated. Hence, it is useful to consider the case where τ_F is taken to be proportional to τ, that is

$$\tau = \alpha\tau_F \tag{9.21}$$

with $\alpha \geq 1$. From the Nyquist criterion, optimal filtering is achieved when $\alpha \simeq 1$. Now, when $\tau \gg \tau_T$, one obtains from Eq. (9.18)

$$\begin{aligned}\langle[\phi_F(t+\tau)-\phi_F(t)]^2\rangle = {} & \frac{D_{N2}}{\alpha}[\alpha-1+e^{-\alpha}][1+\tau_T^2(\omega-\gamma A^2)(\omega-3\gamma A^2)]^2\tau + \alpha D_{N2}(1-e^{-\alpha})\frac{\tau_T^2}{\tau} \\ & + \frac{(D_{N1}+D_D+D_L)}{\alpha}[\alpha-1+e^{-\alpha}][1+\tau_T^2(\omega-3\gamma A^2)^2]\tau \\ & + \alpha D_{N2}(1-e^{-\alpha})[1-2\tau_T^2(\omega-\gamma A^2)(\omega-3\gamma A^2)]\frac{\tau_T^2}{\tau} + \alpha D_F(1-e^{-\alpha})\frac{\tau_T^2}{\tau} . \end{aligned} \tag{9.22}$$

It is thus seen that with optimal filtering the variance in the phase difference decreases as τ^{-1} for small τ. When τ becomes sufficiently large the variance in the phase difference again grows as τ. Thus the frequency uncertainty

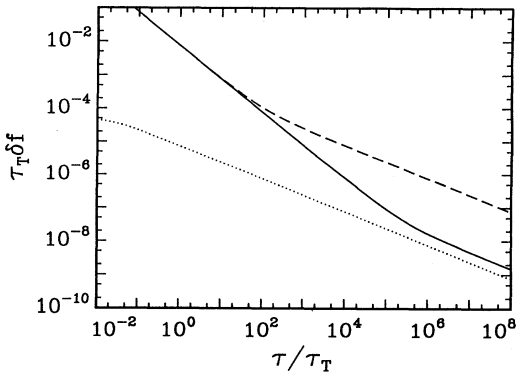

FIG. 7. Frequency stability of the oscillator plotted as a function of the frequency counter time interval. This figure is similar to Fig. 5 except here the counter receives the amplifier's output after passing through a filter with fixed bandwidth. At short times the solid and the dashed curves scale as τ^{-1} due to the broadband noise emitted from the output of the amplifier. See the text for the parameter values used.

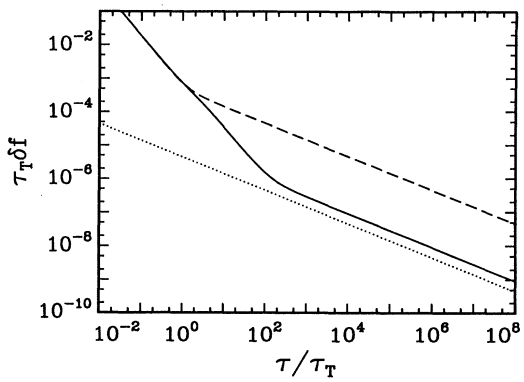

FIG. 8. Frequency stability of the oscillator plotted as a function of the frequency counter time interval. This figure is similar to Figs. 5 and 7 except here the counter receives the amplifier's output after passing through an optimized filter. That is, the filter bandwidth is taken to be equal to the reciprocal of the frequency counter time interval τ. Now at short times the dashed and solid curves scale as $\tau^{-3/2}$ and approach the intrinsic phase stability of the oscillator more rapidly than in Fig. 7. Parameters have been chosen so that this figure can be directly compared with Fig. 5 and Fig. 7. See the text for the parameter values used.

δf scales as $\tau^{-3/2}$ for small τ and as $\tau^{-1/2}$ for large τ. With optimal filtering one can reach much more quickly the diffusive regime determined by the oscillator noise sources.

This behavior is displayed in the plots of δf as a function of τ in Fig. 8. These curves are plots of Eq. (9.17) with $D_F = 0$ and $\tau_F = \tau$. This corresponds closely to the optimized filter. Again the parameters for each of the curves are the same as in Figs. 5 and 7. Note the smaller values for $\tau_T \delta f$ at large τ in Fig. 8, compared to Fig. 7, which reflect the more stringent filtering.

X. A SPECIFIC RESONATOR: THE VIBRATING BEAM

The precise meaning of each of the quantities appearing in Eqs. (2.1)–(2.7) is not always obvious for a particular resonator, especially if the resonator is a distributed object. In this section the correspondence is made between these general quantities and the specific physical quantities characterizing a vibrating beam.

The beam of uniform cross section is assumed to lie along the x axis. Vibration of the beam in the direction of the y axis is governed by the wave equation

$$m\frac{\partial^2 y}{\partial t^2} + EI\frac{\partial^4 y}{\partial x^4} = 0 \ , \tag{10.1}$$

where m denotes the mass per unit length along the beam and

$$F_y = EI\frac{\partial^4 y}{\partial x^4} \tag{10.2}$$

is the elastic restoring force per unit length in the y direction. Here E is the elastic modulus of the material. The moment of inertia I is defined by

$$I = \int_A y^2 dy dz \ , \tag{10.3}$$

where the integration is carried out over the cross-sectional area A of the beam with the center of mass located at $y = 0$. In particular, for a rectangular beam of width W (dimension along the z axis) and height H (dimension along the y axis) one has

$$I = \frac{WH^3}{12} \ . \tag{10.4}$$

The beam length will be denoted by L and the x axis origin will be located at the center of the beam. With the ends of the beam rigidly clamped, the boundary conditions are

$$y = 0 \text{ at } x = \pm L/2 \tag{10.5}$$

and

$$\frac{\partial y}{\partial x} = 0 \text{ at } x = \pm L/2 \ . \tag{10.6}$$

For simplicity we consider only the lowest vibration mode of the beam which has the form

$$y_1(x,t) = c_1 u_1(x)\cos(\omega_1 t + \phi_1) \ , \tag{10.7}$$

where

$$u_1(x) = N_1[\cosh(\eta_1)\cos(k_1 x) - \cos(\eta_1)\cosh(k_1 x)] \ . \tag{10.8}$$

We will postpone until later the choice of normalization constant N_1. The constant k_1 is given by

$$k_1 = \frac{2\eta_1}{L} \tag{10.9}$$

and the eigenfrequency ω_1 is given by

$$\omega_1 = \left(\frac{EI}{m}\right)^{1/2} k_1^2 \ . \tag{10.10}$$

The eigenvalue η_1 is the first nonzero root of the equation

$$\tan\eta = -\tanh\eta \tag{10.11}$$

and has the approximate value

$$\eta_1 = 2.365\,0204 \ . \tag{10.12}$$

The quantities c_1 and ϕ_1 are integration constants.

Including tension and damping, the wave equation for the resonator driven by a Lorentz force is

$$m\frac{\partial^2 y}{\partial t^2} + \alpha\frac{\partial y}{\partial t} + EI\frac{\partial^4 y}{\partial x^4} - T\frac{\partial^2 y}{\partial x^2} = f_L + BI_R \ . \tag{10.13}$$

Here α is the coefficient friction per unit length, T is the tension along the beam, f_L the fluctuating force per unit length associated with the damping, B is the magnetic induction in the z direction, and I_R is the current flowing along the beam. We will refer to the current as the resonator current. The boundary conditions Eq. (10.5) and (10.6) are again imposed, and the tension is taken to be that which arises due to the length change of the beam as the beam is deflected from its equilibrium position. The change in length ΔL of the beam is given by

$$\Delta L = \int_{-L/2}^{L/2} \sqrt{1 + \left(\frac{\partial y}{\partial x}\right)^2}\, dx - L \ . \tag{10.14}$$

For small displacements the square root can be expanded and, to a good approximation, one has

$$\Delta L = \frac{1}{2}\int_{-L/2}^{L/2} \left(\frac{\partial y}{\partial x}\right)^2 dx \ . \tag{10.15}$$

The strain ϵ_x along the beam is given by

$$\epsilon_x = \frac{\Delta L}{L} \ . \tag{10.16}$$

The stress σ_x along the beam is related to the strain through

$$\sigma_x = E\epsilon_x \ . \tag{10.17}$$

Since the stress is the force per unit area, the tension along the beam is given by

$$T = A\sigma_x = AE\frac{\Delta L}{L} \ . \tag{10.18}$$

Substituting Eq. (10.15) into this equation and substituting the result into Eq. (10.13) one obtains

$$m\frac{\partial^2 y}{\partial t^2}+\alpha\frac{\partial y}{\partial t}+EI\frac{\partial^4 y}{\partial x^4}-\frac{AE}{2L}\left[\int_{-L/2}^{L/2}\left(\frac{\partial y}{\partial x'}\right)^2 dx'\right]\frac{\partial^2 y}{\partial x^2}$$

$$=f_L+BI_R\ . \quad (10.19)$$

We also note that the voltage developed along the beam due to its motion through the magnetic field is

$$V_R=B\int_{-L/2}^{L/2}\frac{\partial y}{\partial t}dx\ . \quad (10.20)$$

We now assume that the damping, drive, and tension are small so that the spatial shape of the lowest mode of vibrations is still given by Eq. (10.8). To account for changes in motion due to time varying driving forces we generalize Eq. (10.7) to

$$y(x,t)=Y(t)u_1(x)\ , \quad (10.21)$$

where

$$Y(t)=c_1(t)\cos[\omega_1 t+\phi_1(t)]\ . \quad (10.22)$$

Here $c_1(t)$ and $\phi_1(t)$ are regarded as slowly varying functions of time. Equation (10.20) can now be written as

$$V_R=\ell B\frac{dY}{dt}\ , \quad (10.23)$$

where

$$\ell=\int_{-L/2}^{L/2}u_1(x)dx\ . \quad (10.24)$$

Note that Eq. (10.23) is identical to Eq. (2.7). Multiplying both sides of Eq. (10.19) by $u_1(x)$ and integrating with respect to x from $-L/2$ to $L/2$, one obtains

$$M\frac{d^2Y}{dt^2}+\mu_T\frac{dY}{dt}+K_1Y+K_3Y^3=F_L+\ell BI_R\ , \quad (10.25)$$

where

$$M=m\int_{-L/2}^{L/2}u_1^2(x)dx\ , \quad (10.26)$$

$$\mu_T=\alpha\int_{-L/2}^{L/2}u_1^2(x)dx\ , \quad (10.27)$$

$$K_1=EIk_1^4\int_{-L/2}^{L/2}u_1^2(x)dx\ , \quad (10.28)$$

$$K_3=\frac{AE}{2L}\left[\int_{-L/2}^{L/2}\left(\frac{\partial u_1(x)}{\partial x}\right)^2 dx\right]^2\ , \quad (10.29)$$

and

$$F_L=\ell f_L\ . \quad (10.30)$$

Writing the resonator current I_R as

$$I_R=I_{DS}+I_{AN}\ , \quad (10.31)$$

substituting this equation into Eq. (10.25), and using Eqs. (2.3) and (2.4) one obtains Eq. (2.2). To check if the energy contained in the resonator and the above defined quantities are consistent with Eq. (3.6), consider the kinetic energy of the resonator

$$\mathcal{E}_K=\frac{m}{2}\int_{-L/2}^{L/2}\left(\frac{\partial y}{\partial t}\right)^2 dx\ . \quad (10.32)$$

By substituting Eq. (10.21) into this equation and making use of Eq. (10.26) one obtains

$$\mathcal{E}_K=\frac{M}{2}\left(\frac{dY}{dt}\right)^2\ . \quad (10.33)$$

The notation introduced here is, therefore, consistent with that used in earlier sections. Equation (10.24) and Eqs. (10.26)–(10.30) thus provide the relationship between the effective parameters M, μ_T, K_1, K_3, and ℓ and the physical parameters m, α, E, I, A, and L characterizing the beam resonator.

There is considerable freedom in choosing the normalization constant N_1 appearing in Eq. (10.8). If one chooses to take, for example, the effective resonator length ℓ to be equal to the physical length L, then Eq. (10.24) sets the normalization constant through the equation

$$L=\int_{-L/2}^{L/2}u_1(x)dx\ . \quad (10.34)$$

Alternatively, if one chooses to take the effective mass M to be equal to the total mass of the beam mL then the normalization constant is determined by the equation

$$L=\int_{-L/2}^{L/2}u_1^2(x)dx\ . \quad (10.35)$$

This ambiguity in normalization, however, does not affect the physical quantities of interest, as we demonstrate by several examples.

Here we calculate the maximum displacement of the beam at the resonance peak for a given drive current. From Eqs. (3.1) and (3.20) one obtains the following expression for the amplitude ring-down time in terms of the oscillator's quality factor Q and resonant frequency $\omega_1=\Omega_0$:

$$\tau_T=\frac{2Q}{\omega_1}\ . \quad (10.36)$$

Substituting Eq. (3.22) into Eq. (4.6) one obtains

$$f=\frac{\ell I_0 B}{2\sqrt{2M}}\ . \quad (10.37)$$

Substituting these last two equations into the relation between the drive f and the amplitude A at resonance, Eq. (5.20), and making use of Eq. (3.2) one obtains

$$A = \frac{\ell Q B I_0}{\sqrt{2K_1}} \ . \tag{10.38}$$

Since the amplitude A was chosen to be the square root of the total energy, Eq. (3.5), and since the total energy is equal to the maximum value of the kinetic energy it is easy to show from Eq. (10.33) and Eq. (10.22) that

$$A = \left(\frac{K_1}{2}\right)^{1/2} c_1 \ . \tag{10.39}$$

Eliminating A from Eqs. (10.38) and (10.39) leads to the following expression for the constant c_1 at resonance:

$$c_1 = \frac{\ell Q B I_0}{K_1} \ . \tag{10.40}$$

Since the maximum excursion of the beam occurs at its center $x = 0$, one has from Eqs. (10.21) and (10.22)

$$y_{max} = c_1 u_1(0) \ . \tag{10.41}$$

Combining Eqs. (10.40) and (10.41) and using Eqs. (10.9), (10.24), and (10.28) one obtains

$$y_{max} = \kappa_1 \frac{Q B I_0 L^4}{EI} \ , \tag{10.42}$$

where the constant κ_1 is given by

$$\kappa_1 = \frac{u_1(0)\int_{-L/2}^{L/2} u_1(x)dx}{2^4 \eta_1^4 \int_{-L/2}^{L/2} u_1^2(x)dx} = 2.626 \times 10^{-3} \ . \tag{10.43}$$

Note that κ_1 is independent of the undetermined normalization constant N_1. The numerical value for κ_1 follows from Eqs. (10.8), (10.9), (10.11), and Eq. (10.12), from which one obtains

$$u_1(0) = N_1[\cosh(\eta_1) - \cos(\eta_1)] = 6.0824 N_1 \ , \tag{10.44}$$

$$\begin{aligned}\int_{-L/2}^{L/2} u_1(x)dx &= \frac{2N_1 L}{\eta_1}\cosh(\eta_1)\sin(\eta_1) \\ &= 3.1821 N_1 L \ ,\end{aligned} \tag{10.45}$$

and

$$\begin{aligned}\int_{-L/2}^{L/2} u_1^2(x)dx &= \frac{N_1^2 L}{2}[\cosh^2(\eta_1) + \cos^2(\eta_1)] \\ &= 14.668 N_1^2 L \ .\end{aligned} \tag{10.46}$$

Using Eq. (10.43), Eq. (10.42) can be written

$$y_{max} = 2.636 \times 10^{-3} \ \frac{Q B I_0 L^4}{EI} \tag{10.47}$$

which gives the relation between I_0, the zero-to-peak value of the drive current, and the peak displacement y_{max} of the beam at resonance.

We now evaluate the zero-to-peak voltage V_R^{max} that is developed across the conductor when the peak displacement of the resonator is y_{max}. From Eq. (10.22) and Eq. (10.23) one obtains

$$V_R^{max} = \omega_1 c_1 \ell B \ . \tag{10.48}$$

Using Eq. (10.41) this equation becomes

$$V_R^{max} = \frac{\ell}{u_1(0)} \omega_1 B y_{max} \ . \tag{10.49}$$

The quantity $\ell/u_1(0)$ is independent of the normalization constant N_1 and can be evaluated using Eqs. (10.24), (10.44), and (10.45). One obtains

$$\frac{\ell}{u_1(0)} = 0.52316 L \ , \tag{10.50}$$

leading to the result

$$V_R^{max} = 3.287 f_1 L B y_{max} \ . \tag{10.51}$$

The oscillation frequency f_1 in the above equation is related to the angular frequency through $\omega_1 = 2\pi f_1$.

The expression for the damping time τ_D, Eq. (3.22),

$$\tau_D = \frac{2MR_D}{\ell^2 B^2} \ , \tag{10.52}$$

can now be written in terms of the physical parameters. Making use of Eqs. (10.26) and (10.50) together with Eqs. (10.44) and (10.46) one obtains

$$\tau_D = 2.897 \frac{mLR_D}{L^2 B^2} \ . \tag{10.53}$$

Finally, we calculate the critical drive current beginning with the expression for the critical drive force, Eq. (5.30), which, when combined with Eq. (10.36), can be written

$$f^2 = \frac{\sqrt{3}}{9\gamma}\left(\frac{\omega_1}{Q}\right)^3 \ . \tag{10.54}$$

This force is related to the drive current by Eq. (10.37), and so we have for the critical current

$$I_0 = \frac{2^{3/2}}{3^{3/4}\ell B}\left(\frac{M}{\gamma}\right)^{1/2}\left(\frac{\omega_1}{Q}\right)^{3/2} \ . \tag{10.55}$$

To cast this expression into the desired form, an expression for γ, defined by Eq. (3.19), in terms of the physical quantities characterizing the beam resonator is now obtained. The nonlinear spring constant K_3 appearing in Eq. (3.19) can be written

$$K_3 = 1.5264 \times 10^4 \ N_1^4 \frac{AE}{L^4} \ . \tag{10.56}$$

This relation follows from Eq. (10.29) using the result

$$\begin{aligned}\int_{-L/2}^{L/2}\left(\frac{\partial u_1(x)}{\partial x}\right)^2 dx &= \frac{2N_1^2\eta_1}{L}\{\eta_1[\cosh^2(\eta_1) \\ &\quad - \cos^2(\eta_1)] + 2\cosh^2(\eta_1) \\ &\quad \times \sin(\eta_1)\cos(\eta_1)\} \\ &= 174.72\frac{N_1^2}{L} \ .\end{aligned} \tag{10.57}$$

Using Eq. (10.56) and Eqs. (10.26), (10.28), (10.45), and (10.46), Eq. (3.19) then becomes

$$\gamma = 4.751 \left(\frac{A}{\rho E I^3}\right)^{1/2} L \,. \tag{10.58}$$

Equation (10.55) can thus be written

$$I_0 = 0.6851(\rho^3 E A I^3)^{1/4} \left(\frac{\omega_1}{Q}\right)^{3/2} \,. \tag{10.59}$$

This is the expression for the zero-to-peak drive current I_0 at the critical point in terms of the physical parameters characterizing the resonator.

XI. SUMMARY

It is generally accepted that the optimum frequency stability for a self-excited oscillator is *always* achieved by employing a linear resonator and by operating at resonance, i.e., with the phase at 90°. This paper demonstrates, however, that this is not the case if the feedback amplifier's output noise is significant. There is then an advantage in using a resonator with a cubic nonlinearity and operating at a special point defined by a unique drive and a phase setting of 120°. At this critical point the phase-versus-frequency curve is locally vertical, implying that here the frequency is insensitive to small variations in the phase of the drive. Since amplifier output noise leads to jitter in the phase of the drive, one might, therefore, have anticipated our finding that the consequences of this noise can be evaded by operating at the critical point.

Noise from the amplifier's input port and broadband noise on the excitation signal drive the resonator directly. Consequently, the oscillator's performance with respect to these noise sources is not improved by operating at the critical point. The effect of these noise sources can, however, be reduced by weakening the coupling of the resonator with the amplifier and with the drive. When these couplings are made negligible, the long-term stability of the nonlinear oscillator at its critical point is

$$\delta f = \frac{1}{\pi}\sqrt{\frac{D_L}{\tau}} \,, \tag{11.1}$$

i.e., the fluctuations in the frequency now are due only to noise associated with the resonator's intrinsic losses.

The corresponding result for the oscillator based on a *linear* resonator is

$$\delta f = \frac{1}{2\pi}\sqrt{(D_{N2} + D_L)/\tau} \tag{11.2}$$

which now includes the term D_{N2} describing phase diffusion due to amplifier output noise. When D_{N2} is small compared to D_L, Eqs. (11.1) and (11.2) differ by a factor of 2, meaning that the nonlinear system is more responsive to loss noise. Consequently, the benefits of using the nonlinear system are realized only if D_{N2} is at least a factor of 3 larger than D_L.

Equations (11.1) and (11.2) are two special cases of the general expression, Eq. (9.17), for the frequency fluctuations, which is the main result of this paper. This expression gives the frequency fluctations of a self-excited oscillator operating at any point along a linear or nonlinear resonance curve.

Although a simple nonlinear mechanical resonator was treated in detail as a specific example, the general principles are also applicable to many other types of oscillators. Among them would be electrical oscillators, where the required nonlinearity might be provided by a varactor diode capacitor, and optical oscillators, where the nonlinearity might be provided by a Kerr medium whose index of refraction varies as the square of the intensity.

[1] V. B. Braginsky, Usp. Fiz. Nauk. **154–156**, 93 (1988) [Sov. Phys. Usp. **31**, 836 (1988)].

[2] D. S. Greywall, B. Yurke, P. A. Bush, A. N. Pargellis, and R. L. Willett, Phys. Rev. Lett. **72**, 2992 (1994) and (unpublished).

[3] B. Yurke and A. N. Pargellis (unpublished).

[4] V. B. Braginsky, Y. I. Vorontsov, and K. S. Thorne, Science **209**, 547 (1980).

[5] C. M. Caves, K. S. Thorne, R. W. P. Drever, V. D. Sandberg, and M. Zimmermann, Rev. Mod. Phys. **52**, 341 (1980).

[6] C. M. Caves, in *Squeezed and Nonclassical Light*, edited by P. Tombesi and E. R. Pike (Plenum, New York, 1989), pp. 29–38.

[7] D. Rugar and P. Grütter, Phys. Rev. Lett. **67**, 699 (1991).

[8] M. F. Bocko and W. W. Johnson, Phys. Rev. A **30**, 2135 (1984).

[9] W. H. Press, B. P. Flannery, S. A. Teukolsky, and W. T. Vetterling, *Numerical Recipes in C* (Cambridge University Press, Cambridge, 1988), p. 157.